

**ENHANCED DUAL-BAND PLANAR INVERTED-F ANTENNA FOR  
WLAN APPLICATIONS**

**By**

**Sana Fayeq Aref Salameh**

**Supervisor**

**Dr. Mohamed K. Abdelazeez**

**This Thesis was Submitted in Partial Fulfillment of the  
Requirements for the Master's Degree of Science in  
Electrical Engineering/Communication**

**Faculty of Graduate Studies  
The University of Jordan**

**August, 2009**

## COMMITTEE DECISION

This Thesis (Enhanced Dual-Band Planar Inverted-F Antenna for WLAN Applications) was successfully Defended and Approved on 5-8-2009

### Examination Committee

### Signature

Dr. Mohammed K. Abdelazeez, (Supervisor)  
Prof. of Electrical Engineering

*m.k. abdelazeez*

*Dr. Dia I. Abu Al-Nadi*  
*Assoc. Prof. of Electrical Engineering*

*Dia Abunnadi*

*Dr. Nizar M. Zorba*  
Assist. Prof. of Electrical Engineering

*[Signature]*

Dr. Omar R. Asfar  
Prof. of Electrical Engineering  
(Jordan University of Science and Technology)

*O. Asfar*

تعتمد كلية الدراسات العليا  
هذه النسخة من الرسالة  
التوقيع..... التاريخ ١٤/٥/٢٠٠٩

## Dedication

*To my mother and father*

*to my spouse and daughter, and to all who support me.*

## Acknowledgement

I wish to express deepest gratitude and sincere thanks to my supervisor; Professor Mohamed K. Abdelazeez for his encouragement, invaluable guidance, advice and help with which the completion of this work becomes possible.

Also I want to thank Dr.Loay Khalaf and Al-Bahith group for technology for their help in performing the measurements.

## List of Contents

Committee Decision.....	ii
Dedication.....	iii
Acknowledgment.....	iv
List of Contents.....	v
List of Figures.....	vii
List of Abbreviations.....	xi
Abstract(in the language of the of the thesis).....	xii
<b>1. Introduction.....</b>	<b>1</b>
<b>1.1 Motivation.....</b>	<b>1</b>
<b>1.2 Aim and Scope of the Thesis.....</b>	<b>2</b>
<b>1.3 Previous Studies and Thesis Formulation.....</b>	<b>3</b>
<b>2. The Planar Inverted-F Antenna.....</b>	<b>6</b>
<b>2.1 Basic Planar Inverted-F Antenna Geometry.....</b>	<b>6</b>
<b>2.2 Electric Field Distribution.....</b>	<b>7</b>
<b>2.3 Current Distribution.....</b>	<b>9</b>
<b>2.4 Resonant Frequency.....</b>	<b>11</b>
<b>2.5 Effects of Substrates Parameters and Shorting Posts.....</b>	<b>14</b>
<b>2.6 Consideration for the Planar Inverted-F Antenna.....</b>	<b>14</b>
<b>3. Simulation Results and Discussion.....</b>	<b>16</b>
<b>3.1 Simulation Software.....</b>	<b>16</b>
<b>3.2 Results and Discussion.....</b>	<b>16</b>
<b>3.3 Multiband PIFDLA for WLAN Applications.....</b>	<b>26</b>
<b>3.3.1 The Effect of Short-Circuit Plate Width.....</b>	<b>32</b>

3.3.2 The Effect of Finite Ground Plane Size.....	33
3.3.3 The Effect of Coaxial Cable Length.....	37
3.3.4 The Effect of Substrate.....	37
3.3.5 Measurement Results.....	45
3.4 Multiband PIFDLA for WLAN Application and WiMAX.....	46
4. Conclusions, and Recommendations for Future Work.....	54
5. References.....	56
6. Abstract (in the second language).....	58

## List of Figures

NUMBER	FIGURE CAPTION	PAGE
1	The Geometry of PIFA Antenna	6
2	Distribution of the electric fields $E_x$ , $E_y$ , and $E_z$ at the x-y plane for PIFA	9
3	Surface current distribution on the PIFA for $L_1 = L_2$ .	10
4	Normalized resonant frequency versus normalized shorting plate width $W$ for PIFA in Fig.1	11
5	Variation of surface current flow underneath the planar element due to size ratio of planar element and width of short-circuit plate.	12
6	(a) Geometry of the Planar Inverted F-L Antenna (b) side view of the PIFLA	17
7	The Return loss of the PIFLA using HFSS	19
8	The Return loss of the PIFLA using CST, IE3D, and measurement	19
9	The Return loss of PIFLA for different ground plane thicknesses	20
10	The Effect of the short-circuit plate width	21

11	The Effect of feed plate location	22
12	PIFLA with slot in the short-circuit plate of inverted-F antenna	22
13	Return loss for PIFLA with slot in the short-circuit plate of inverted-F	23
14	PIFLA with slot in the short-circuit plate of inverted-L antenna	23
15	Return loss for PIFLA with slot in the short-circuit plate of inverted-L antenna	24
16	PIFLA with slot between feed plate and short-circuit plate	25
17	Return loss for PIFLA with slot between feed plate and short-circuit plate	25
18	The Geometry of PIFDLA	29
19	The Return loss for PIFDLA of F-patch 6 mm above the ground plane	30
20	The Radiation pattern for the PIFDLA of F-patch 6 mm above the ground plane (a) with respect to $\theta$ for $\phi = 0^\circ$ and $\phi = 90^\circ$ at 2.5 GHz (b) with respect to $\theta$ for $\phi = 0^\circ$ and $\phi = 90^\circ$ at 5.67 GHz (c) with respect to $\phi$ for $\theta = 90^\circ$ at 2.5 GHz (d) with respect to $\phi$ for $\theta = 90^\circ$ at 5.67 GHz.	30-32
21	The Effect of short-circuit plate width	33



22	The Effect of square finite ground plane on PIFA	34
23	The Return loss of PIFA for rectangular ground plane with $0.25 \lambda$ length in x-axis	35
24	The Return loss of PIFA for rectangular ground plane with $0.25 \lambda$ length in y-axis	36
25	The Return loss for different coaxial cable lengths	37
26	The Geometry of PIFDLA supported by substrate	38
27	The Return loss of PIFDLA with dielectric material as substrate( $\epsilon_r = 1.2$ )	38
28	The Radiation pattern of PIFDLA with $\epsilon_r = 1.2$ substrate (a) with respect to $\theta$ for $\phi = 0^\circ$ and $\phi = 90^\circ$ at 2.48 GHz (b) with respect to $\theta$ for $\phi = 0^\circ$ and $\phi = 90^\circ$ at 5.22 GHz (c) with respect to $\phi$ for $\theta = 90^\circ$ at 2.48 GHz (d) with respect to $\phi$ for $\theta = 90^\circ$ at 5.22 GHz.	39-40
29	The Geometry of PIFDLA supported by substrate with copper thickness 0.17 mm	42
30	The Return loss for PIFDLA supported by substrate with 0.17 mm copper thickness.	42
31	The Radiation pattern for PIFDLA supported by substrate with 0.17 mm copper thickness (a) with respect to $\theta$ for $\phi = 0^\circ$ and $\phi = 90^\circ$ at 2.45 GHz (b) with respect to $\theta$ for $\phi = 0^\circ$ and $\phi = 90^\circ$ at 5.35 GHz (c) with respect to $\phi$ for $\theta = 90^\circ$ at 2.45 GHz (d) with respect to $\phi$ for $\theta = 90^\circ$ at 5.35 GHz.	43-44
32	The Measured Return Loss for PIFDLA of Fig.18	45
33	The VSWR of PIFDLA of Fig.18	46

34	The Return loss for PIFDLA of F-patch 5mm above the ground plane	47
35	The Radiation pattern for PIFDLA of F-patch 5mm above the ground plane (a) with respect to $\theta$ for $\phi = 0^\circ$ and $\phi = 90^\circ$ at 2.57 GHz (b) with respect to $\theta$ for $\phi = 0^\circ$ and $\phi = 90^\circ$ at 5.44 GHz (c) with respect to $\phi$ for $\theta = 90^\circ$ at 2.57 GHz (d) with respect to $\phi$ for $\theta = 90^\circ$ at 5.44 GHz.	47-49
36	The Return loss for PIFDLA of F-patch 5mm above the ground plane with substrate $\epsilon_r=1.2$	50
37	The Radiation pattern for PIFDLA of F-patch 5mm above the ground plane supported by substrate (a) with respect to $\theta$ for $\phi = 0^\circ$ and $\phi = 90^\circ$ at 2.5 GHz (b) with respect to $\theta$ for $\phi = 0^\circ$ and $\phi = 90^\circ$ at 5.19 GHz (c) with respect to $\phi$ for $\theta = 90^\circ$ at 2.5 GHz (d) with respect to $\phi$ for $\theta = 90^\circ$ at 5.19 GHz.	50-52

## List of Abbreviations

CST	Computer Simulation Technology
DSSS	Discrete Sequence Spread Spectrum
HFSS	High Frequency Structure Simulator
IE3D	Integral Equation, three Dimensions
IFA	Inverted-F Antenna
OFDM	Orthogonal Frequency Division Multiplexing
PCs	Personal Computers
PIFA	Planar Inverted-F Antenna
PIFDLA	Planar Inverted-F Dual-L Antenna
PIFLA	Planar Inverted-F-L Antenna
SAR	Specific Absorption Rate
SNM	Special Network Method
VSWR	Voltage Standing Wave Ratio
WiMAX	Worldwide Interoperability for Microwave Access
WLAN	Wireless Local Area Network

# ENHANCED DUAL-BAND PLANAR INVERTED-F ANTENNA FOR WLAN APPLICATIONS

By  
**Sana Fayege Aref Salameh**

Supervisor  
**Dr. Mohamed K. Abdelazez**

## ABSTRACT

Wireless local area networks (WLANs), connecting portable terminals such as laptop computers, have recently seen a great growth. The use of WLANs is governed through standardization of frequency bands defined by various standard protocols, namely, Bluetooth, IEEE 802.11a/b/g and HIPERLAN2. The need for devices to operate in all WLANs frequency bands is driving research toward the design of multiband radiating antennas. Additionally, the small space available in such terminals requires the design of high performance elements that must be small, light, and highly compatible with all of the electronic devices integrated in the same mobile terminal. Planar inverted-F antennas (PIFAs) are among the most used radiating elements for mobile terminals, since they can be modified to obtain multi-frequency bands. In this thesis, a new multiband single-feed planar inverted-F dual-L antenna (PIFDLA) is presented. This proposed antenna simultaneously operates in the IEEE 802.11b/g (2.4 GHz-2.484 GHz) or WiMAX band (2.5 GHz-2.7 GHz), IEEE 802.11a (5.15GHz-5.35GHz, 5.725 GHz-5.825 GHz), and HIPERLAN2 (5.47 GHz-5.725 GHz). The simulation for this multiband single-feed antenna has been carried out using high frequency structure simulator software (HFSS) to investigate the antenna's performance and characteristics. The simulation results will demonstrate that the antenna can operate at the above desired resonant frequencies.

## CHAPTER 1 INTRODUCTION

The rapid growth of local area network (WLAN) applications has created strong demands for small internal antennas. Due to the limited space availability in the wireless devices, the design of low cost and small size antennas is required. In current wireless environments, there are many wireless devices working in several frequency bands, and providing different services. There is an increasing need to provide many wireless services with one device. An example of this is the integration of Bluetooth, mobile phone, and wireless local area network (WLAN) capabilities into some laptop computers. However, this normally requires many antennas to cover these services, and it is not possible to fit them all in a small device. To address this requirement, antennas that operate in multiple bands have been developed. One family of such antennas, the planar-inverted-F antennas (PIFAs), are particularly interesting due to their compactness and suitable performance.

### 1.1 Motivation

With the rapid development of personal computers (PCs) and the desire of users to transmit/receive information between PCs over the air, WLAN nowadays has been widely applied for many aspects. Since 1999, the WLAN standards including IEEE 802.11a/b/g systems were established by IEEE 802.11 Group. In the USA, the 802.11b/g WLAN standards are used for the frequency range from 2.4 to 2.4835 GHz as the 802.11a standards are used from 5.15 to 5.35 GHz (indoor) and 5.725 to 5.825 GHz (outdoor). In practical applications, the 802.11b system was first implemented utilizing the direct-sequence spread spectrum (DSSS) modulation scheme with the data rate up to 11 Mbps, yet the 802.11g system for higher transmission data rate (up to 54 Mbps) was done later

through the same frequency band as the 802.11b but with orthogonal frequency division multiplexing (OFDM) modulation scheme (Wang, et al., 2007). Being a key component of the wireless network system, the antenna has gotten so much attention and improvement, especially in capability and size.

## 1.2 Aim and Scope of the Thesis

There are many wireless devices working in several frequency bands providing different services. There is an increasing need to provide many wireless services in one device such as integration of Bluetooth, mobile phone and WLAN applications into some laptop computers. However, this normally requires many antennas to cover these bands, and it is not possible to fit them all in a small device. To address this requirement, antennas that operate in multibands have been developed. The idea is to enhance the functionality and performance of wireless communication devices and to cover the existing wireless communication frequency bands. PIFA antenna has been adopted in portable wireless units due to its low profile and ability to cover the existing wireless communication frequency bands. Due to limited space availability in wireless devices, the purpose is to keep the size of the antenna small and appropriate for portable wireless units without degrading the performance in terms of bandwidth and radiation patterns; so the antenna design should be as omni-directional as possible to cover the required operating frequency bands for the IEEE 802.11a/b/g standard. In this thesis we will modify the PIFA to enhance its bandwidth and size for WLAN applications.

The objectives of this thesis are accomplished with the steps listed below;

- Research on various internal multiband antenna designs; study and understand each antenna characteristics.

- Select a suitable antenna design to form the basis for the thesis. Study and understand the antenna theory and characteristics.
- With good understanding of PIFA, design a new antenna to operate in the required frequency bands. Simulations are carried out to determine the performance of the antenna.
- Investigate the new antenna characteristics and compare obtained results with published work.

### 1.3 Previous Studies and Thesis Formulation

The conventional PIFA is widely used because of several advantages such as matching the input impedance with no outer circuit, low profile, small overall size, and having omnidirectional radiation pattern. However, its length is limited to be a quarter-wavelength of the operating frequency, which usually occupies small space in the PCB. Besides, the single PIFA can only operate at a certain resonant frequency, which is unable to supply the market need of dual-band or triple-band applications. So many dual-band antennas have been proposed; some of these designs use two similar resonators to achieve dual-band operations, such as double inverted-F antenna, dual-U shaped monopole, double-L monopole, monopole with parasitic plane, etc (Wang, et al., 2007 ). Each design describes antenna shape and size and gives simulation and measurement results for antenna gain, return loss and radiation pattern. All antenna designs differ in antenna size, PCB size, antenna gain, bandwidth that the antenna covers, and the radiation pattern of the designed antenna. Two novel printed inverted-F antennas (PIFA) for 2.45 GHz and 5.25 GHz WLAN applications were introduced; one is designed by spiraling the tail of the PIFA and the results show that it has 10 dB return loss with bandwidth of 140 MHz centered at 2.45

GHz and bandwidth of 756 MHz centered at 5.25 GHz, the other is by modifying the feed structure of the PIFA into coupling configuration and it has bandwidth of 240 MHz around 2.45 GHz and bandwidth of 672 MHz around 5.25 GHz (Wang, et al., 2007). In another study, a dual-band planar inverted-F antenna (PIFA) presented to cover both 2.4 GHz and 5 GHz bands used in all IEEE 802.11 WLAN standards; in that study a PIFA was modified to achieve a wider 10-dB return loss bandwidth in the upper frequency band than the lower band, and the measured results showed that the 10-dB return loss bandwidth obtained was 2.4 - 2.5 GHz (4%) and 4.5 - 6.25 GHz (32.5%), another thing to be considered is that the size of the ground plane in that study was 48 mm × 40 mm (Esselle, et al., 2008 ). In another study a PIFA was introduced to cover both 2.4 GHz and 5 GHz for WLAN applications, in this study a compromise between size reduction and attainable bandwidth was provided. From simulated and measured results an optimum (minimized) volume of 30 mm×30 mm×8 mm gave 8% bandwidth at the lower resonant mode of 2.4 GHz, while at the higher resonant mode of 5.5 GHz a bandwidth of 12.2% is obtained (Zhou, et al., 2008). Also new class of miniature printed embedded inverted-F antennas proposed for operation in the 2.4-2.485 GHz WLAN band; the proposed antennas which is on FR4 substrate (dielectric constant=4.4) measured 9.2 mm by 4.1 mm and has a bandwidth of 3.5%. The peak gain of this antenna was 1.4 dBi and an overall size reduction of 70% was achieved compared to a conventional inverted-F antenna (Azad and Ali, 2006). Another paper presented a numerical study on the effects of human head on the PIFA operating at 2.45 GHz. The PIFA was placed at the side of the head; and the radiation patterns and gain were compared in free space and on the human head (Looi).



In this thesis basic planar inverted-F antenna (PIFA) geometry, characteristics, electric field distribution, current distribution, resonant frequency, bandwidth, radiation pattern, impedance matching, effect of shorting posts, effect of substrates and antenna efficiency are introduced in Ch.2. Simulation software (HFSS), simulation results and discussions including return loss curves, radiation patterns for each frequency band of multiband single-feed planar inverted-F dual-L antenna operating on IEEE 802.11a/b/g, Bluetooth and HIPERLAN2 frequency bands are given in Ch.3. In Ch.4, conclusions and recommendations for future work are presented.

## CHAPTER 2

### THE PLANAR INVERTED-F ANTENNA

#### 2.1 Basic Planar Inverted-F Antenna Geometry

The planar inverted-F antennas (PIFA) typically consists of a rectangular planar element, ground plane, and short-circuit plate. The PIFA is an inverted-F antenna (IFA) with the wire radiator element replaced by a flat conducting plate oriented parallel to the ground plane as shown in Fig.1. The PIFA is widely applied as a low profile antenna design.

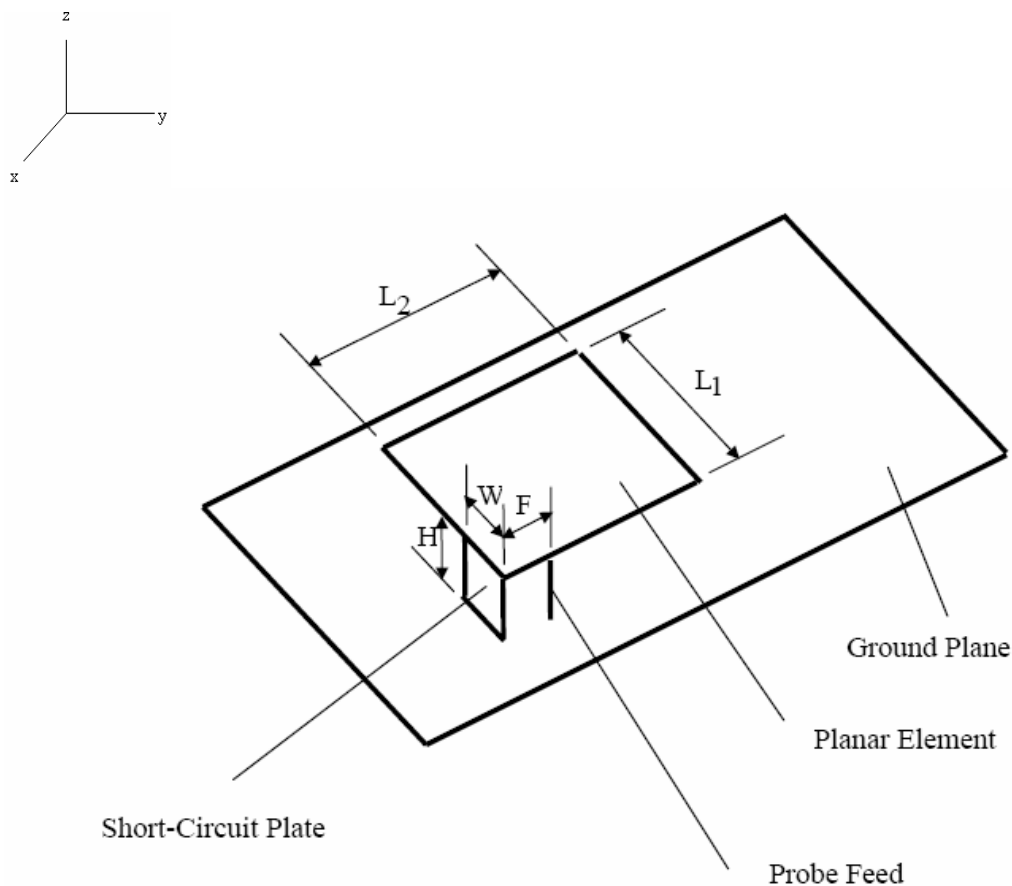


**Figure 1:** The Geometry of the PIFA Antenna

The PIFA in Fig.1 consists of a planar element with a probe feed. The feed line is coaxial with the outer conductor connected to the ground plane and the center conductor emerging from beneath the ground plane to contact the planar element. One edge of the PIFA is shorted to ground using a plate of width  $W \leq L_1$ . The resonant frequency of the PIFA depends upon the width of the short-circuit plate,  $W$ , the height of the element,  $H$ , and the dimensions of the planar element,  $L_1$  and  $L_2$ .

The parameters of the PIFA can be adjusted by varying the dimensions with respect to others.

- An increase in  $H$  widens the bandwidth.
- Reducing  $W$  ( $W < L_1$ ) reduces the overall dimension and also the bandwidth.
- $L_2$  allows frequency tuning.
- Every modification changes the position of the feed point for given impedance.

## 2.2 Electric Field Distribution

The dominant component of the electric field  $E_z$  is equal to zero at the short-circuit plate while the intensity of this field at the opposite edge of the planar element is significantly large. The peaked part of the electric field distributions  $E_x$  and  $E_y$  are located at the feed point. Also, the electric fields are generated at all open circuited edges of the planar element. These fringing fields are the radiating sources in PIFAs. Fig.2 illustrates the distribution of the electric fields  $E_x$ ,  $E_y$ , and  $E_z$  computed using the spatial network method (SNM), which is a three-dimensional time-domain numerical analysis method (Shibita, et al., 1988), for different cases where the width of the short-circuit plate is

changed as  $2\Delta d, 4\Delta d, 8\Delta d$  and  $12\Delta d$ , respectively, when the planar element has the size of  $L_1 = L_2 = 16\Delta d$  and  $H = 4\Delta d$ , where  $\Delta d$  is the interval of spatial discretization, when the antenna is broken up into three-dimensional cubical grid whose length is  $\Delta d$ . The result shows clearly that the dominant electric field  $E_z$  is zero at the short-circuit plate, and the peaked parts of the electric field distributions  $E_x$  and  $E_y$  are located at the feed point. Also, the electric fields are generated at all open circuited edges of the planar element (Hirisawa, et al., 1992).

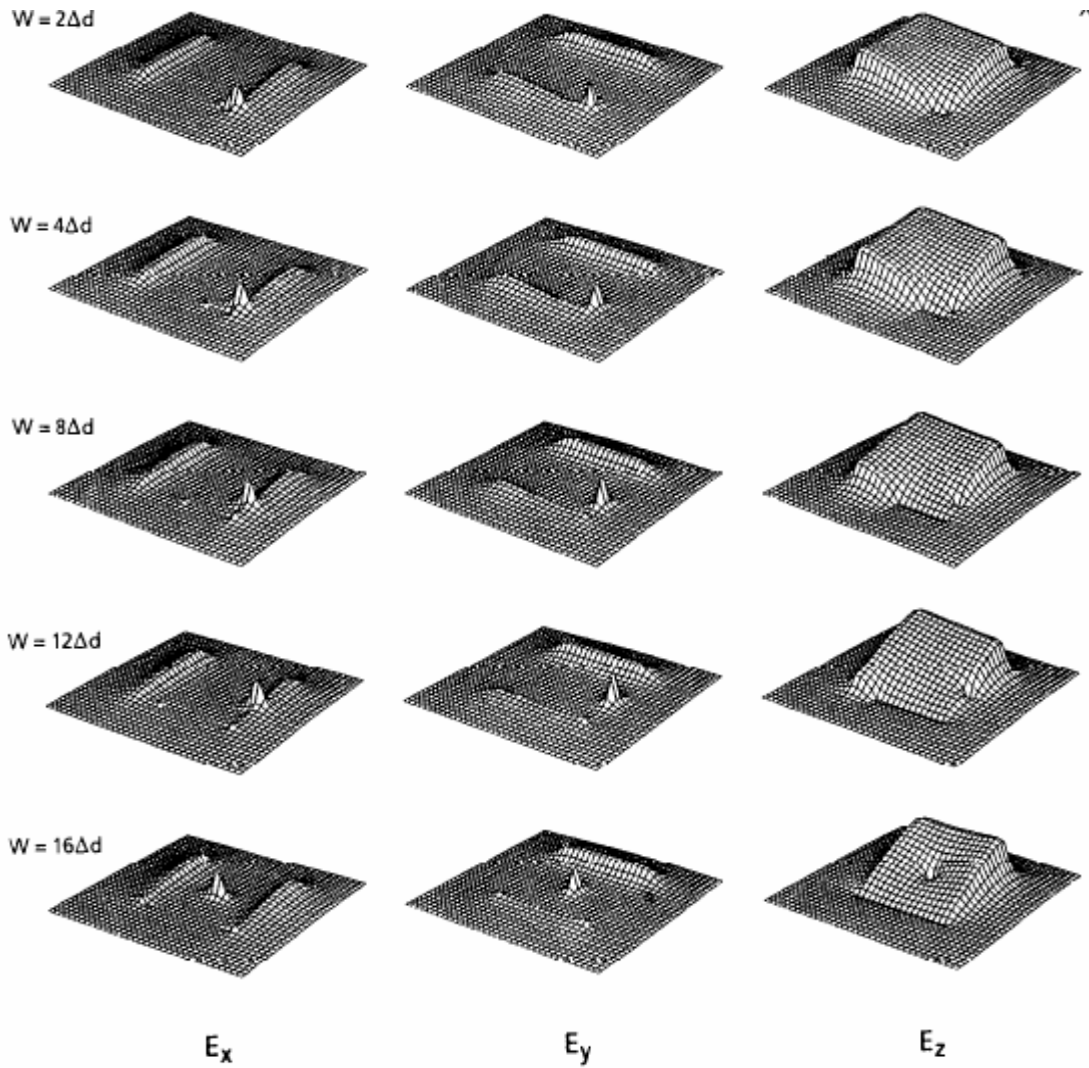


**Figure 2:** Distribution of the electric fields  $E_x$ ,  $E_y$ , and  $E_z$  at the x-y plane, where observed plane is at the height of  $2.5\Delta d$  from the ground plane for  $E_z$  field and  $2\Delta d$  for  $E_x$  and  $E_y$  fields computed using SNM (Hirisawa, et al., 1992).

### 2.3 Current Distribution

PIFA has very large current flows on the undersurface of the planar element and the ground plane. These currents contribute to the interior electric and magnetic fields between the planar element and the ground plane. The intensity of the current on the upper surface of

the planar element is relatively small. Due to this behavior PIFA is one of the best candidates when we talk about the influence of external objects that affect the antenna characteristics (e.g. mobile operator's hand/head). When the width of the short-circuit plate is narrowed, the current distribution changes and the effective length of the current flow on the short-circuit plate and planar element becomes longer. Consequently, the resonant frequency is reduced (Hirisawa, et al., 1992). Fig.3 shows the current distribution intensity: the upper, middle, and lower distributions show the surface current on the upper surface, the underneath surface of the planar element, and the ground plane respectively.

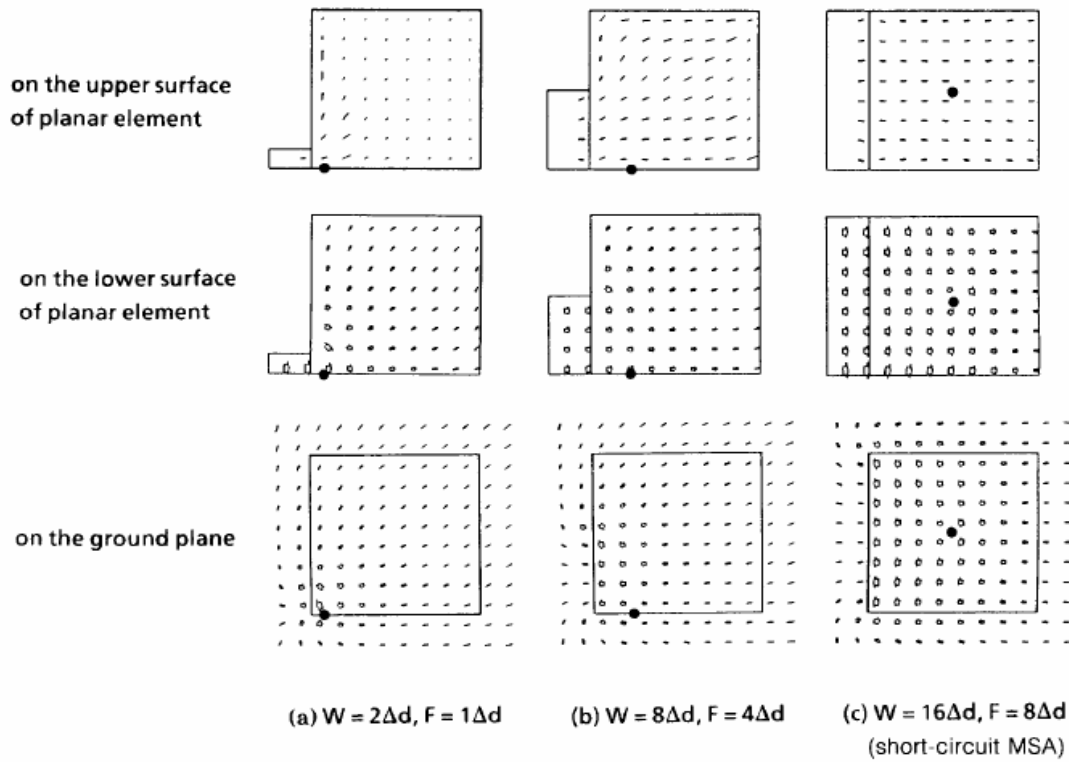


**Figure 3:** Surface current distribution on the PIFA for  $L_1 = L_2$ . The black dot shows the feed points (Hirisawa, et al., 1992).

## 2.4 Resonant Frequency

The resonant frequency depends on the width of the short-circuit plate  $W$ . To see this effect, simulations were performed by (Hirisawa, et al., 1992) on a PIFA for various short-circuit plate widths with the following dimensions:  $L_1 = L_2 = 16\Delta d$ ,  $H = 2\Delta d$ ,  $\Delta d = 4\text{mm}$ ; the result of this simulation is shown in Fig.4. The frequency  $f_1$  is the resonant frequency when  $W = L_1$ . As predicted, the resonant frequency  $f_r$  decreases by decreasing the width  $W$ .

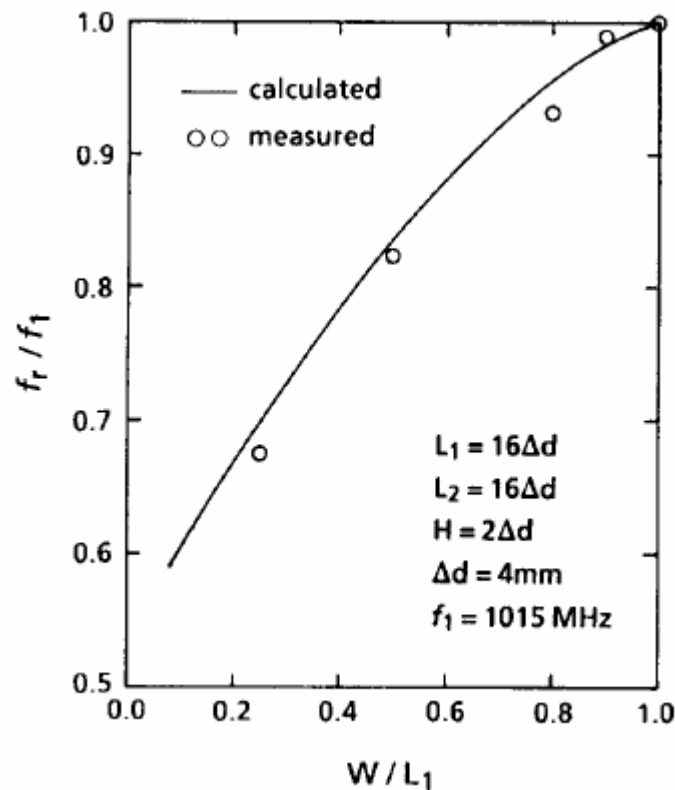


**Figure 4:** Normalized resonant frequency versus normalized shorting plate width  $W$  for PIFA in Fig.1.  $f_1$  is the resonant frequency for PIFA with dimensions  $W = L_1$ . Data were computed using SNM (Hirisawa, et al., 1992).

The PIFA resonant frequency  $f_r$  is also influenced by the size ratio of the planar element,  $L_1/L_2$ . Results show that as the plate width  $L_1$  increases (as measured by  $L_1/L_2$ ) the resonant frequency decreases, i.e.,  $f_r/f_1$ , for a fixed  $W$ , the resonant frequency of the PIFA is proportional to the effective length of the current distribution (Hirisawa, et al., 1992). The variation of surface current flow underneath the planar element due to the size ratio of planar element and width of short-circuit plate is shown in Fig.5.

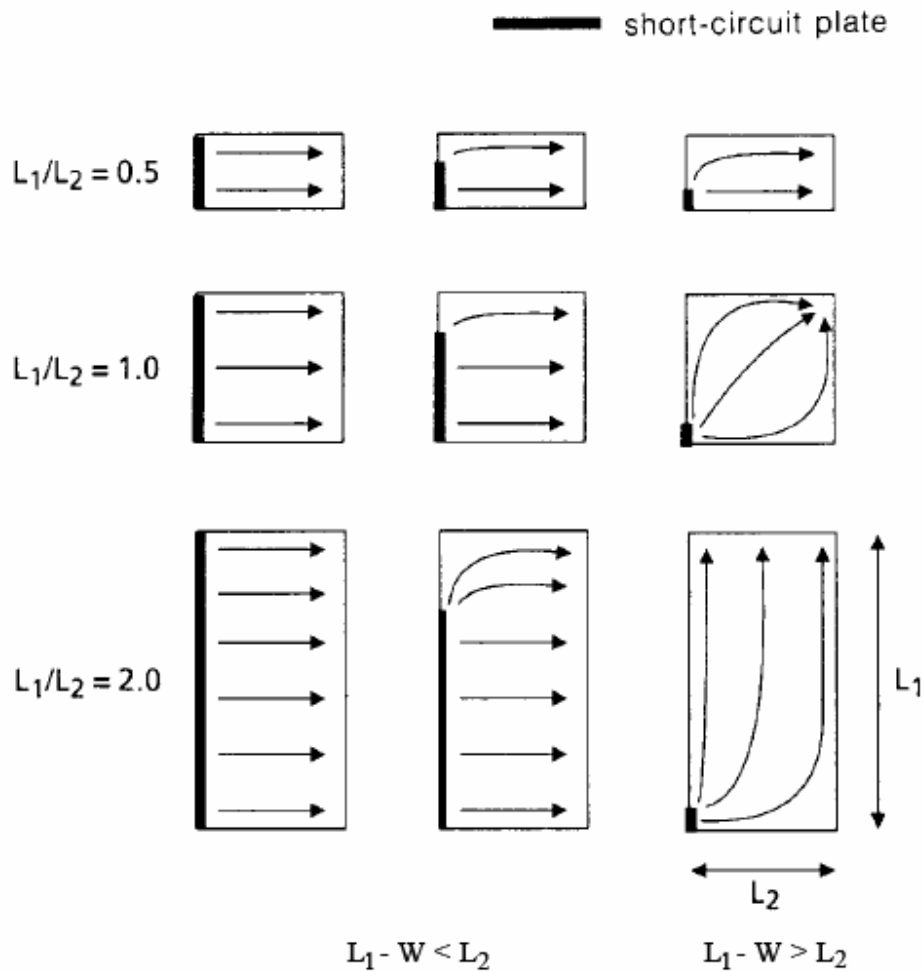


**Figure 5:** Variation of surface current flow underneath the planar element due to size ratio of planar element and width of short-circuit plate (Hirisawa, et al., 1992).



There are two cases in which it is easy to formulate an expression of the resonant frequency with respect to the size of the PIFA (Hirisawa, et al., 1992). The first case is when the width of the short-circuit plate  $W$  is equal to the length of the planar element; say  $L_1$ . This is a quarter-wavelength antenna. The effective length for this case is  $L_2 + H$ , where  $H$  is the height of the short-circuit plate. The resonant condition is then expressed by

$$L_2 + H = \frac{\lambda}{4} \quad (1)$$

where  $\lambda$  is the wavelength. The resonant frequency associated with  $W = L_1$  is

$$f_1 = \frac{c}{4(L_2 + H)} \quad (2)$$

where  $c$  is the speed of light. The other case is for  $W = 0$ . A short-circuit plate with a width of zero can be physically represented by a thin short pin. The effective length of the current is then  $L_1 + L_2 + H$ . For this case, the resonant frequency is expressed by

$$f_2 = \frac{c}{4(L_1 + L_2 + H)} \quad (3)$$

The bandwidth of a PIFA depends on a few parameters, specially the size ratio of the planar element  $L_1 / L_2$ , the height of the short-circuit plate  $H$ , and the ratio  $W / L_1$ . The bandwidth increases with the height of the short-circuit plate and with the size ratio of the planar element  $L_1 / L_2$ . Bandwidth decreases with the decrease of the short-circuit plate width (Hirisawa, et al., 1992).

## 2.5 Effects of Substrate Parameters and Shorting Posts

Impedance bandwidth of the PIFA is inversely proportional to the quality factor ( $Q = \text{Energy Stored} / \text{Power Lost}$ ). Substrates with high dielectric constant  $\epsilon_r$  tend to store energy more than radiate it. This is equivalent to modeling the PIFA as a lossy capacitor with high  $\epsilon_r$ , thus leading to high  $Q$  value and obviously reducing the bandwidth. Similarly when the substrate thickness is increased the inverse proportionality of thickness to the capacitance decreases the energy stored in the PIFA and the  $Q$  factor also. In summary, the increase in height and decrease of  $\epsilon_r$  can be used to increase the bandwidth of the PIFA (Mueiz, 2006).

The shorting posts can be analyzed by modeling them as short pieces of a transmission line of length  $l$ , where  $l$  is the height from the ground plane to the conducting patch. Therefore the shorting posts will add inductance and capacitance to the antenna structure. The series inductance is the total self-inductances of all shorting posts whereas capacitance is due to the close proximity of the shorting posts. The values of inductance and capacitance depend on the number of the shorting posts, their radius, separation between the centers, the permeability and permittivity of the substrate (Mueiz, 2006).

## 2.6 Consideration for the Planar Inverted-F Antenna

Small volume, good electrical characteristic make PIFA a promising candidate for the mobile phone and communication applications in addition to the following considerations:

- Dimensions of conducting patch: they depend on the design frequency.
- Size of the ground plane: ground plane affects the bandwidth to a greater extent; it

should be optimized for the design frequency.

- Position of the feed: it plays a major role in impedance matching; the position of the feed should be as close to the short in order to get good impedance matching.
- The efficiency of PIFA in its environment is reduced by all losses including: ohmic losses, mismatch losses, feed line transmission losses, edge power losses, external parasitic resonances, etc.
- The radiation pattern of the PIFA is the relative distribution of radiated power as a function of direction in space. In the usual case the radiation pattern is determined in the far-field region and is represented as a function of directional coordinates.

## CHAPTER 3

### SIMULATION RESULTS AND DISCUSSIONS

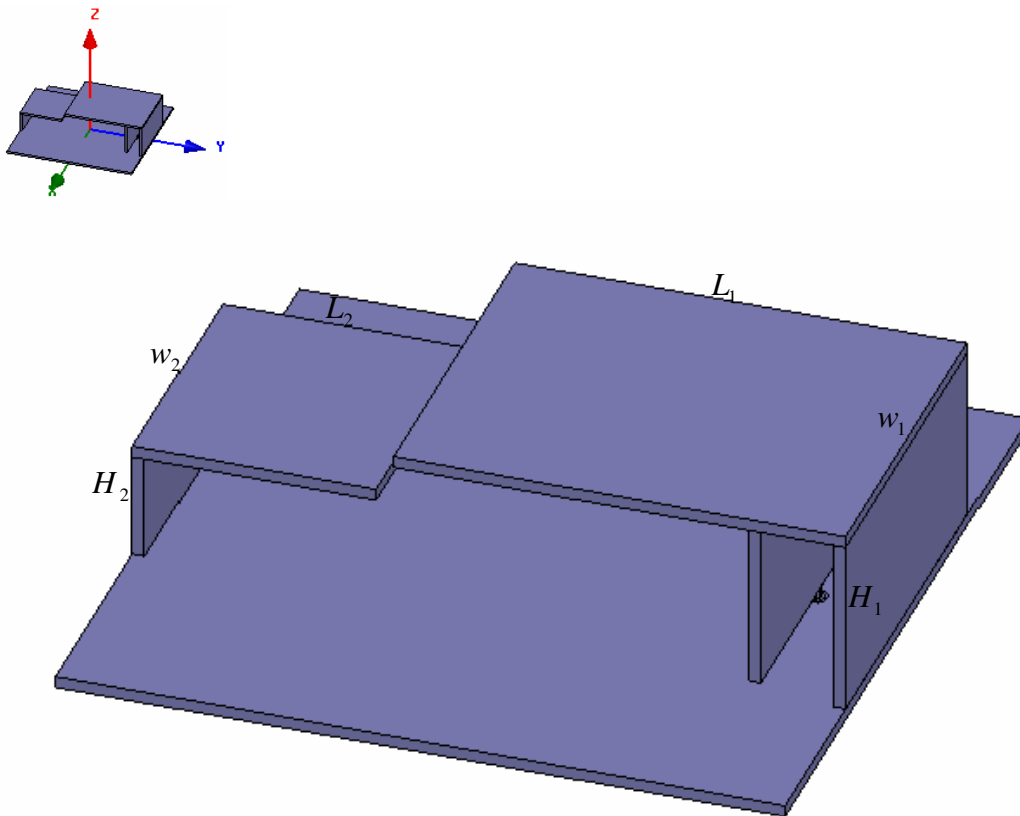
#### 3.1 Simulation Software

The software used to model and simulate the PIFA is Ansoft High Frequency Structure Simulator (HFSS). HFSS is an attractive software package for calculating the electromagnetic behavior of a structure. It allows the design of three-dimensional (3D) high frequency structures such as connectors, IC packages and antennas found in cellular telephones, broadband communication systems, and microwave circuits. It also performs a full-wave finite element electromagnetic analysis. It can be used to calculate and plot the  $S$  parameters, Voltage Standing Wave Ratio (VSWR), current distributions, and radiation pattern of an antenna. Hence, HFSS is widely used in the electromagnetic (EM) and Radio Frequency (RF) industries.

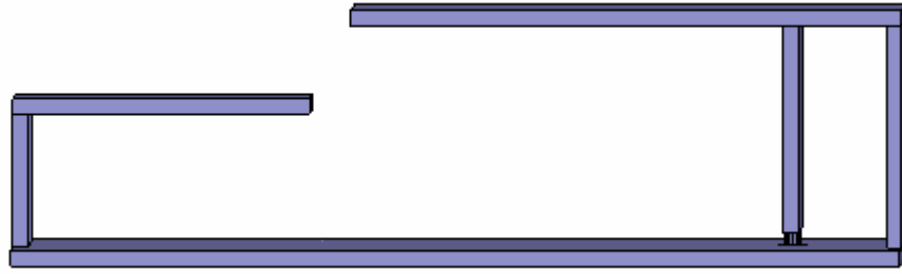
#### 3.2 Results and Discussions

The design of multi-band PIFA is not easy due to the characteristics of the PIFA, which are very sensitive to dimension changes and the effect of ground plane. Although much of its operation and characteristics are already known, it does not mean that everything is understood about the design of the PIFA. In fact, many current methods of PIFA design in practical applications are still being done through a trial and error process (Mueiz, 2006). Therefore, a lot of time and patience is required in designing the multi-band PIFA. The criterion of this thesis is to design an efficient, small and low profile PIFA antenna with multi-band operation for WLAN and Bluetooth applications. Thus, to start

with, a lot of studies have been done in this field as mentioned in ch.1, and Fig. 6 shows the geometry of PIFA for one of those studies with overall size of  $30\text{ mm} \times 15\text{ mm} \times 8\text{ mm}$ , mounted on a  $30\text{ mm} \times 30\text{ mm}$  finite ground plane with  $0.5\text{ mm}$  copper conductor thickness,  $L_1 = 18.6\text{ mm}$ ,  $w_1 = 15\text{ mm}$ ,  $H_1 = 8\text{ mm}$ ,  $L_2 = 10\text{ mm}$ ,  $w_2 = 11\text{ mm}$ , and  $H_2 = 5\text{ mm}$ . In this design a modified PIFA is adopted having a rectangular plate element because of its attractive enhanced bandwidth characteristic (Olmos, et al., 2004). This PIFA is modified to operate as dual-band antenna so an inverted-L antenna is added to operate at the desired upper operating frequency for WLAN applications while the inverted-F antenna operates at the desired lower band for Bluetooth.



(a)



(b)

**Figure 6:** (a) Geometry of the Planar Inverted F-L Antenna (b) side view of the PIFLA

This antenna with its characteristics as given in (Zhou, et al., 2008) ( $L_1 = 18.6$  mm,  $w_1 = 15$  mm,  $H_1 = 8$  mm,  $L_2 = 10$  mm,  $w_2 = 11$  mm, and  $H_2 = 5$  mm) is simulated using HFSS. Fig.7 shows the return loss of this antenna using HFSS which is approximately the same as simulated return loss using Computer Simulation Technology (CST) and Integral Equation three Dimensional (IE3D) simulators and measurement results of (Zhou, et al., 2008); it can be clearly seen that two resonant modes are observed at 2.5 GHz and 5.28 GHz. The lower-band from 2.41 GHz to 2.61 GHz at a minimum return loss of -10 dB or less, encompassing the desired IEEE802.11b/g, Bluetooth and ZigBee frequency band (2400-2485 MHz). The upper-band from 5 GHz to 5.66 GHz fully covers the IEEE802.11a (5.15-5.35 GHz) band. Fig. 8 shows the return loss of PIFLA using CST and IE3D simulators in addition to the measurement results (Zhou, et al., 2008) which shows; the lower-band from 2.4 GHz to 2.6 GHz with resonance at 2.5 GHz and a minimum return loss of -10 dB or less, the upper-band from 5 GHz to 5.65 GHz has a resonance frequency at 5.3 GHz.

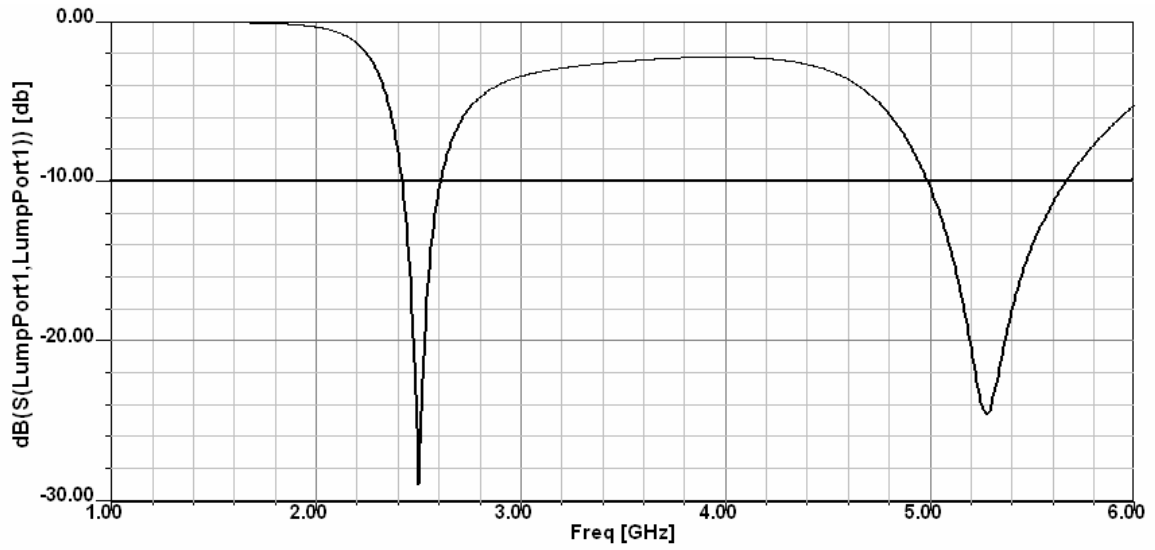


Figure 7: Return Loss of the PIFLA using HFSS.

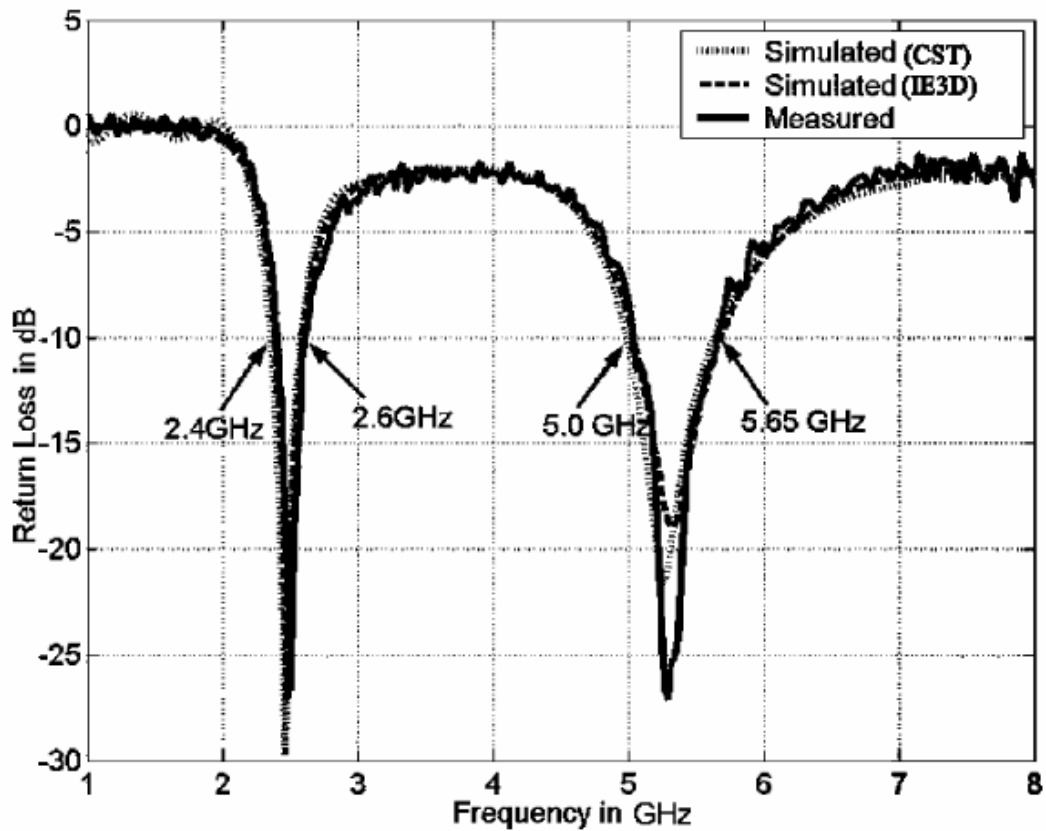
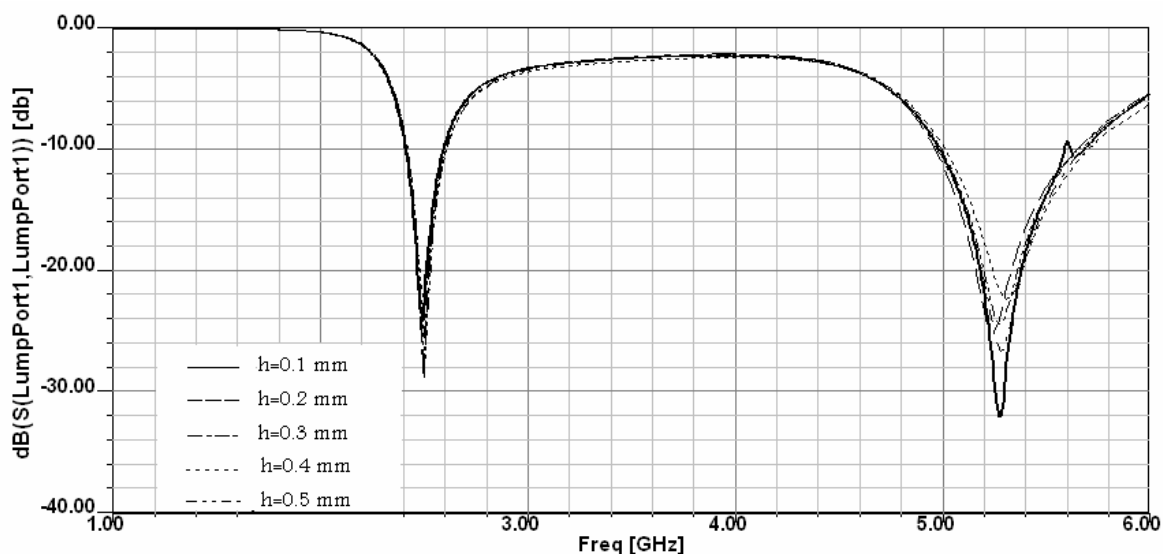


Figure 8: Return Loss of the PIFLA (Zhou, et al., 2008).

Now we aim to enhance the performance of PIFLA of (Zhou, et al., 2008) with respect to bandwidth, radiation pattern, overall size, and/or gain. We want to see the effect of ground plane thickness, width of short-circuit plate, location of feed plate, slots and substrates. By changing the thickness of ground plane  $h$  from 0.1 mm to 0.5 mm as seen in Fig.9; the lower band is still the same for all thicknesses, but for the upper band an enhancement of about 4.5% is obtained at thicknesses of 0.4 mm and 0.3 mm and an enhancement of 3% at thickness of 0.2 mm but the bandwidth is reduced by 7.5% at a thickness of 0.1 mm.



**Figure 9:** The Return Loss for Different Ground Plane Thicknesses.

By changing the width of the short-circuit plate  $w_1$  from 7 mm to 15 mm with step size of 1 mm; for short-circuit plate widths from 7 mm to 11 mm, the return loss at resonance is -10 dB (the reference on which we take the bandwidth for the upper and lower bands) or more for the lower band and it is less than -20 dB for the upper band at short-circuit plate widths from 7mm to 15mm. The best choice for the short-circuit plate width with respect to return



loss and bandwidth is 15 mm (short wall) which is equal to the width of the planar element, because the bandwidth of PIFA decreases as the short-circuit plate width is decreased (Hirisawa, et al., 1992). Fig.10 shows the return loss for short-circuit plate widths of 7 mm, 11 mm, 13 mm, and 15 mm.

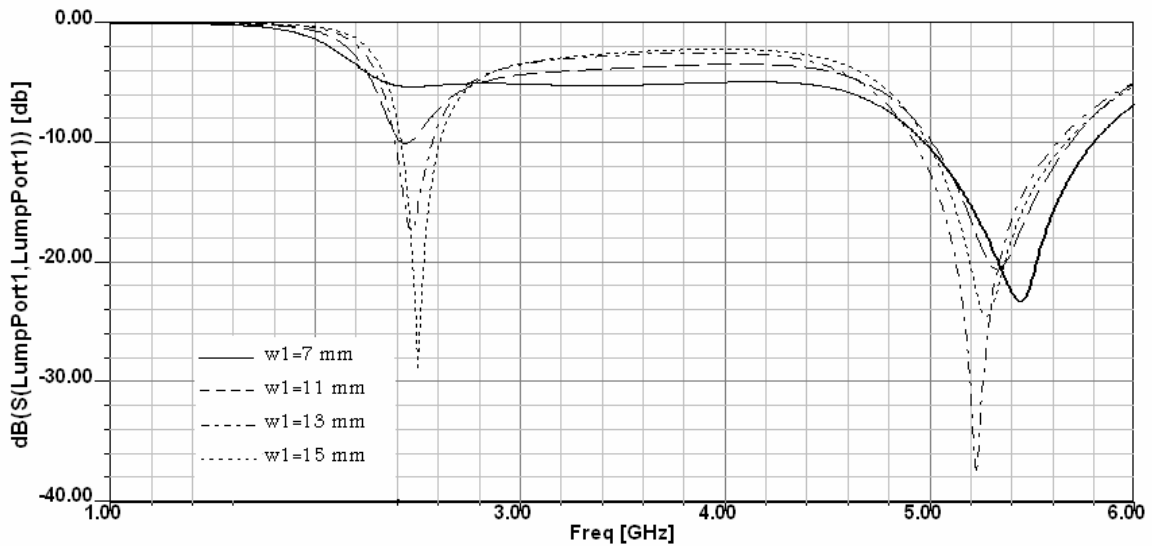


**Figure 10:** The Effect of the Short-Circuit Plate Width.

By changing the distance  $d$  between short-circuit plate and feed plate from 2.5 mm to 6.5 mm with step size of 0.25 mm; for the distances from 4.5 mm to 6.5 mm, the return loss at resonance for the lower band is more than -10 dB in addition to frequency shift for the upper band, so the best location for the feed plate was at distance of 3.5 mm from the short-circuit plate, because the position of the feed plays a major role in the impedance matching (Mueiz, 2006). Fig.11 shows the distances of 6.5 mm, 4 mm, 3.5mm, and 3 mm between short-circuit plate and feed plate.

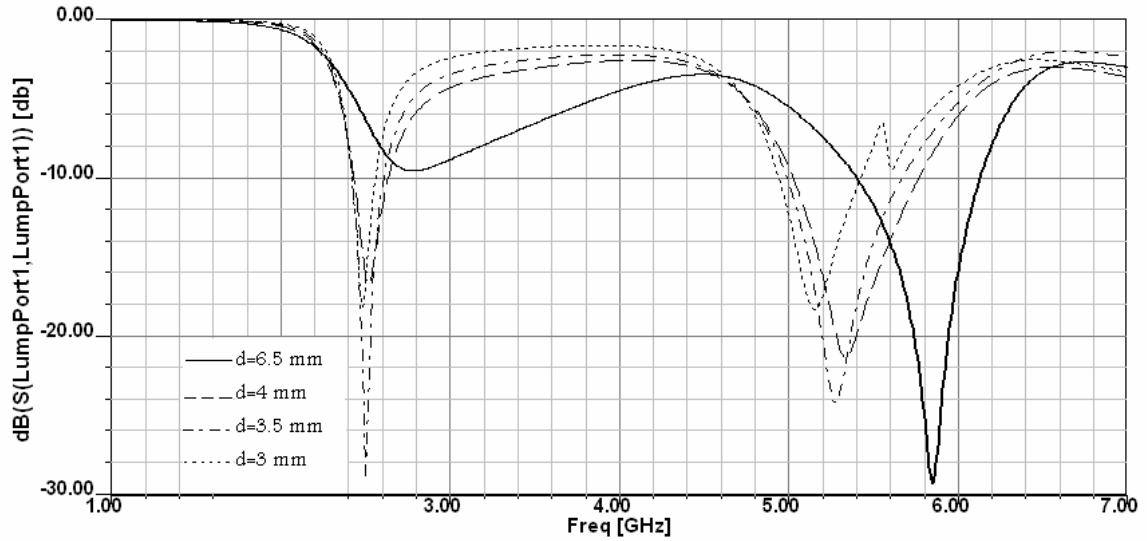


**Figure 11:** The Effect of Feed Plate Location.

By creating a slot in the short-circuit plate of inverted-F antenna with length  $L$  varying from 3mm to 6mm with step size of 1 mm and width of 1 mm as shown in Fig.12, this slot adds no changes to upper or lower bandwidth rather than enhancing the return loss for the upper band to be -32dB for slot of length 6 mm as Fig.13 shows.

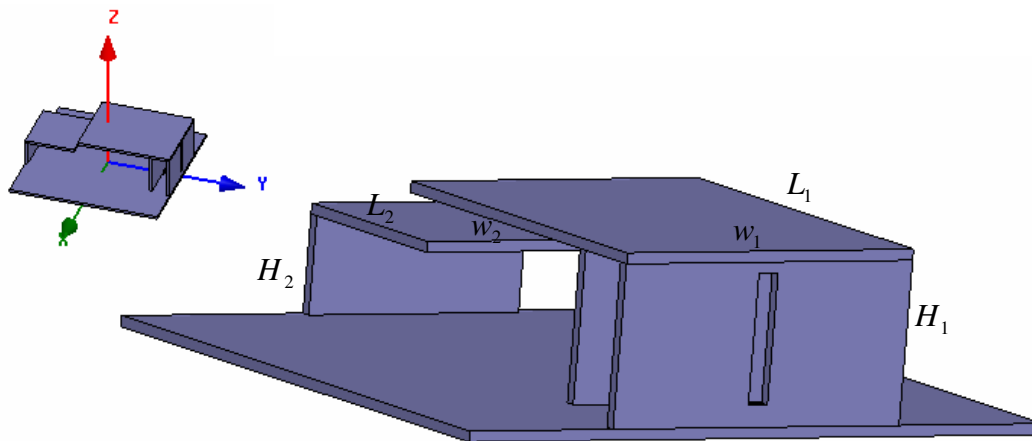


**Figure 12:** PIFLA with Slot in the Short-Circuit Plate of Inverted-F Antenna.

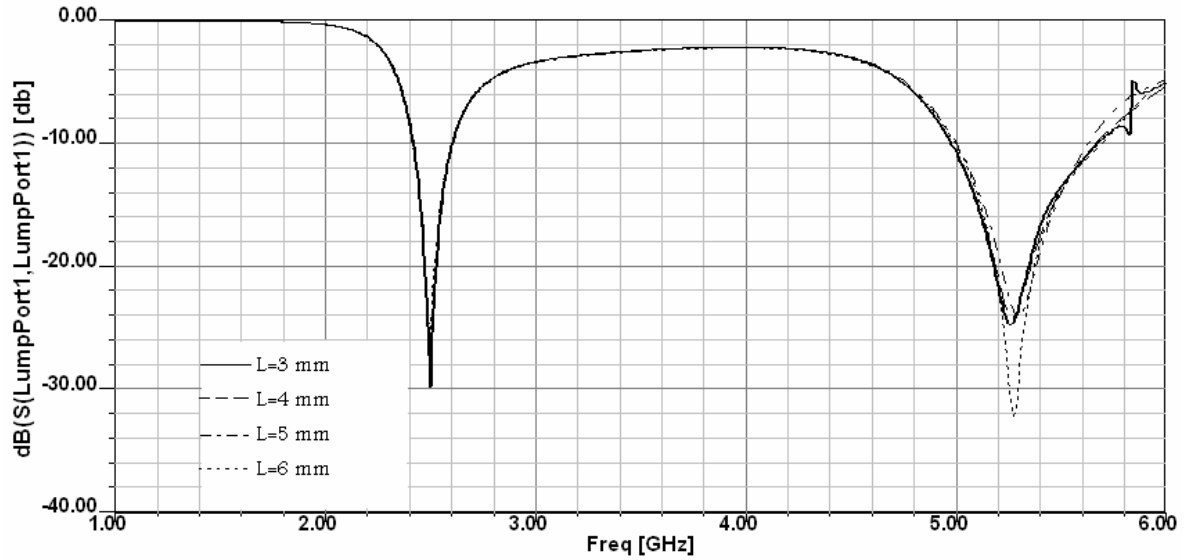


**Figure 13:** Return Loss for PIFLA with Slot in the Short-Circuit Plate of Inverted-F.

By creating a slot in the short-circuit plate of inverted-L antenna with length  $L$  varying from 1 mm to 4 mm of step size of 1 mm and width of 1 mm as shown in Fig.14, there is no bandwidth enhancement for lower or upper band rather than shifting the resonant frequency of the upper band as shown in Fig. 15

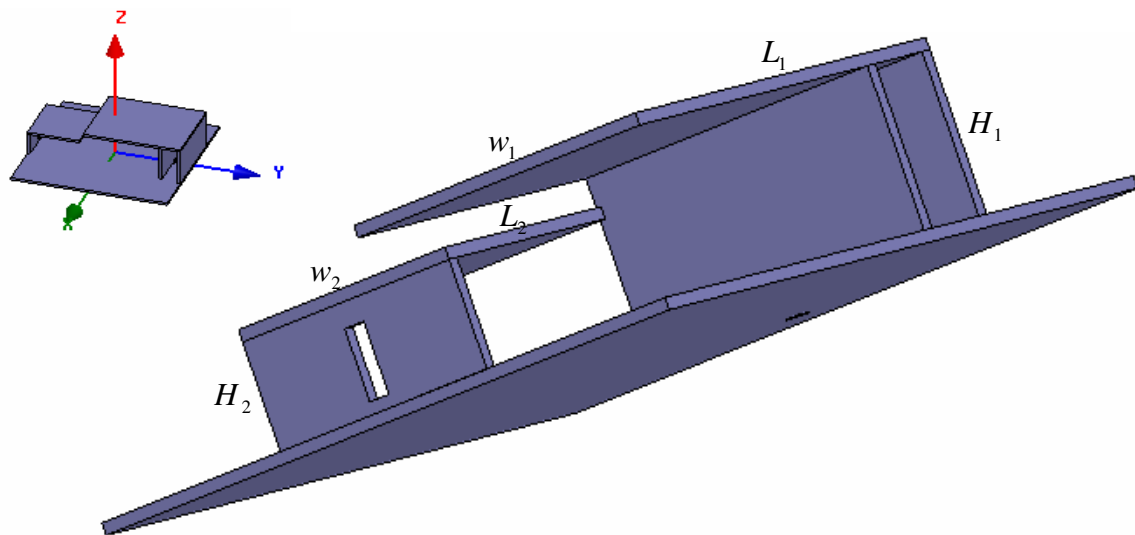


**Figure 14:** PIFLA with Slot in the Short-Circuit Plate of Inverted-L Antenna.

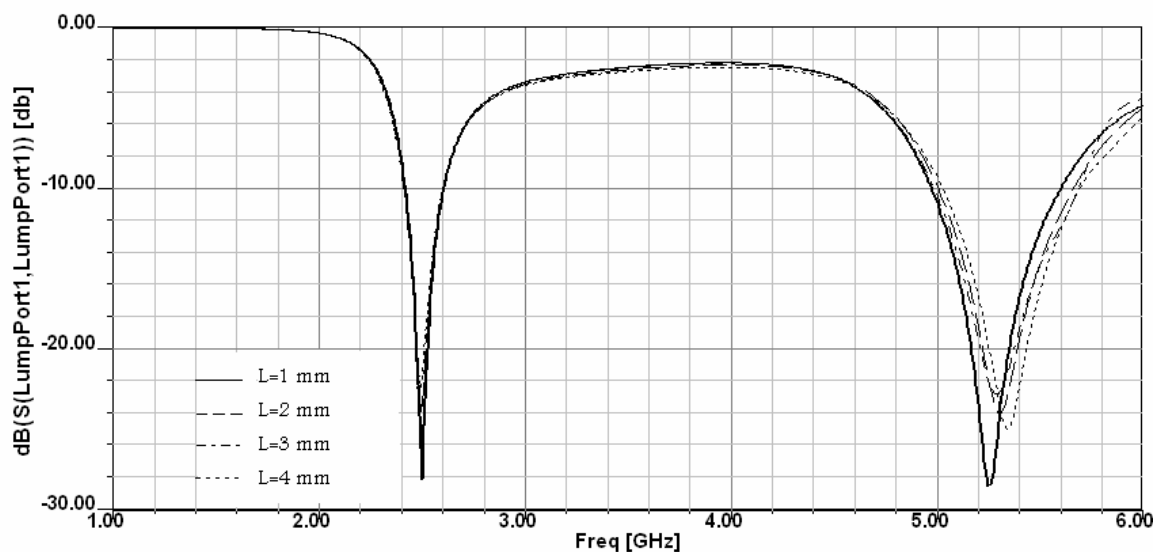


**Figure 15:** Return Loss for PIFLA with slot in the Short-Circuit Plate of Inverted-L Antenna.

By creating a slot in the planar element between feed plate and short-circuit plate with length of 13mm and widths of 0.5 mm, 1 mm, and 2 mm as seen in Fig.16, the results show no enhancement in return loss for the lower band (-13dB or more) for slot of widths 1 mm and 2 mm, but for slot of width 0.5 mm and  $L_1 = 18$  mm,  $w_1 = 15$  mm,  $H_1 = 7.5$  mm,  $L_2 = 9.75$  mm,  $w_2 = 11$  mm, and  $H_2 = 5$  mm, the upper band was enhanced by 12.3% (4.98 GHz-5.71 GHz), and the lower band by 20% (2.49 GHz-2.73 GHz), in addition to the size reduction of 6.25%, as shown in Fig. 17, because slots in the PIFA top plate nominally provide series reactance when the slot opening is close to the feed (Kiven, et al., 2006).

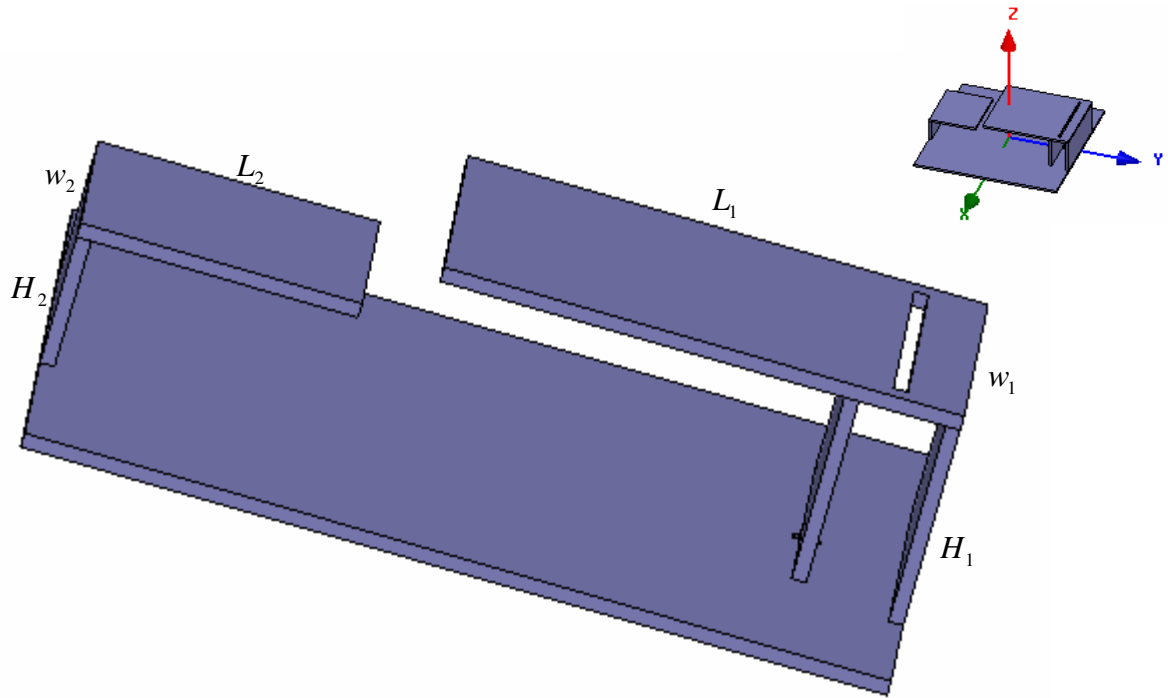


**Figure 16:** PIFLA with Slot between Feed Plate and Short-Circuit Plate.

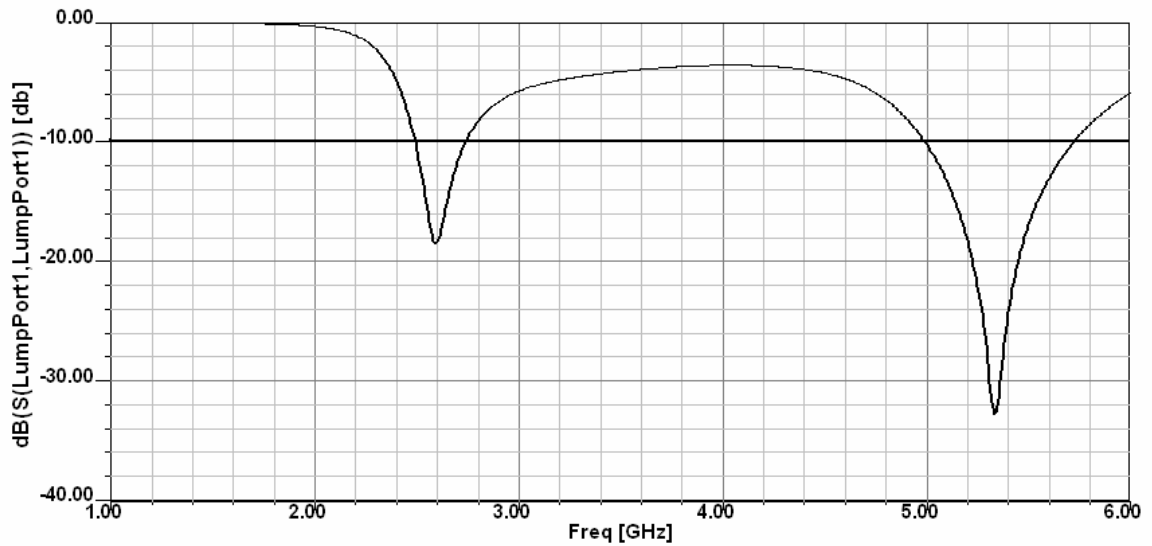


**Figure 17:** Return Loss for PIFLA with Slot between Feed Plate and Short-Circuit Plate.

Because this PIFLA is fragile, we strengthen it by adding substrate; for different thicknesses of FR4 substrate ( $\epsilon_r=4.4$ ), results show no acceptable return loss for FR4 substrate of (30 mm×30 mm) and thickness of 0.6 mm and above. For FR4 substrate of 30 mm×30 mm×0.2 mm and  $L_1 = 18.6$  mm,  $w_1 = 15$  mm,  $H_1 = 7.5$  mm,  $L_2 = 10$  mm,  $w_2 = 11$  mm, and  $H_2 = 5$  mm, the lower band decreased by 5%, and shifted by 10 MHz (2.42 GHz to 2.61 GHz), and the upper band is from 5.0 GHz to 5.69 GHz. Another substrate of dielectric material ( $\epsilon_r=1.2$ ) is used with 30 mm×10 mm× 4.5 mm for inverted-L which is 4.5 mm above the ground plane and 30 mm×20 mm×5 mm for inverted-F which is 5 mm above the ground plane, results show reduction of 30% for the lower band (2.5 GHz-2.64 GHz) in addition to frequency shift from 2.4 GHz to 2.5 GHz, and for the upper band (4.6 GHz-4.9 GHz), it does not cover WLAN applications.

### 3.3 Multiband PIFDLA for WLAN Applications

To solve the problem of fragility for PIFLA of (Zhou, et al., 2008), a Planar Inverted-F Dual-L Antenna (PIFDLA) to be mounted on laptop computers is presented. This proposed multiband single-feed PIFA simultaneously operates in the IEEE 802.11a/b/g, Bluetooth, and HIPERLAN2 frequency bands. The enhancement on upper band and lower band compared with PIFLA of (Zhou, et al., 2008) is due to copper thickness of 1mm and creating slot between feeding plate and short-circuit plate of inverted-F planar element, in addition to using dual inverted-L as parasitic elements instead of using only one inverted-L.

In order to design our proposed antenna we started with PIFLA of 1 mm copper thickness and  $L_1 = 18.6$  mm,  $w_1 = 14.5$  mm,  $H_1 = 7$  mm,  $L_2 = 10$  mm,  $w_2 = 10.5$  mm,  $H_2 = 5.5$  mm mounted on a ground plane of 30 mm × 30 mm × 1 mm. The simulation results for this

antenna that we started with showed an enhancement on the upper band compared with (Zhou, et al., 2008), but gave a bandwidth reduction for the lower band from 200 MHz- which is the lower band of PIFLA in (Zhou, et al., 2008) - to 140 MHz or less in addition to poor return loss for the lower band. To enhance the lower band a slot of 11 mm  $\times$  1.5 mm  $\times$  1 mm is introduced between feeding plate and short-circuit plate of F-patch because slots in the PIFA top plate nominally provide series reactance when the slot opening is close to the feed (Kiven, et al., 2006). This slot enhanced the lower band by 10 MHz to 20 MHz , which is still less than the lower band of the original PIFLA, so we need to adjust all parameters again to obtain enhanced bandwidth for lower band and this is what we obtained but with frequency shift for the lower band. To solve this problem another inverted-L antenna was added. We noticed after many simulations that

1. The length of L-patch  $L_2$  affects the lower band; as the length reduces the lower band increases but with shift; it started after 2.4 GHz for lower band and after 5.15 GHz for the upper band; which means that as the distance between L-patch and F-patch increases, then the bandwidth increases.
2. The distance between the ground plane and the L-patch  $H_2$  compensates for the frequency shift as it increases but reduces the bandwidth of the lower band.
3. The distance between the dual inverted-L and the length of F-patch in y-axis affects the bandwidth and the frequency shift.

The effect of the inverted-L parasitic element on bandwidth enhancement appears through controlling the resistance and reactance between the two resonances to achieve an overall broad-bandwidth (Kathleen, et al., 1997) .We adjusted all these parameters ( $L_1 = 18.4$

mm,  $w_1 = 12$  mm,  $H_1 = 7$  mm,  $L_2 = 9.75$  mm,  $w_2 = 8.5$  mm,  $H_2 = 6.2$  mm) to obtain a compact multiband single-feed PIFA for WLAN applications with 15% enhancement on the lower band (2.4 GHz-2.63 GHz) and 53.8% enhancement on the upper band (5.04 GHz-6.04 GHz) with gain of 7.9 dB, 10.6 dB at 2.5 GHz, and 5.67 GHz respectively in addition to 12.5% size reduction compared with PIFLA of (Zhou, et al., 2008) based on the following calculations; we fixed the resonant frequency  $f_r$  to be 2.5 GHz for the lower band which is created from inverted-F antenna, so the wavelength  $\lambda = 120$  mm. Because the width of the short-circuit plate  $W$  is equal to the width of planar element  $w_1$ , the effective current length is  $H_1 + L_1$  and the resonant condition is  $L_1 + H_1 = \frac{\lambda}{4} = 30\text{mm}$ .

We fixed the height of the F-patch to 6 mm above the ground plane and calculate the planar element length from above relation to be 24 mm, but due to the coupling between inverted-F and inverted-L, the best length for the planar element of inverted-F was 18.4 mm. For the upper band which created from inverted-L antenna, we set the resonant frequency to be 5.67 GHz, and then the wave length is 53 mm.

Because the width of the short-circuit plate for inverted-L antenna  $W$  is equal to the width of L-planar element  $w_2$ , the effective current length is  $H_2 + L_2$ , where  $L_2$  is the length of L-planar element, and  $H_2$  is the height of the short-circuit plate. Then the resonant condition is  $L_2 + H_2 = \frac{\lambda}{4} = 13.25\text{mm}$ .

We fixed the height of the L-patch to 5.2 mm above the ground plane and calculate the L-planar element length from above relation to be 8.05 mm, but due to the coupling between



inverted-F and inverted-L, the best length for the planar element of inverted-L was 9.75mm.

Our final Planar Inverted-F Dual-L Antenna (PIFDLA) is shown in Fig.18. The return loss  $S_{11}$  and radiation pattern for this antenna are shown in Figs. 19, and 20, respectively.

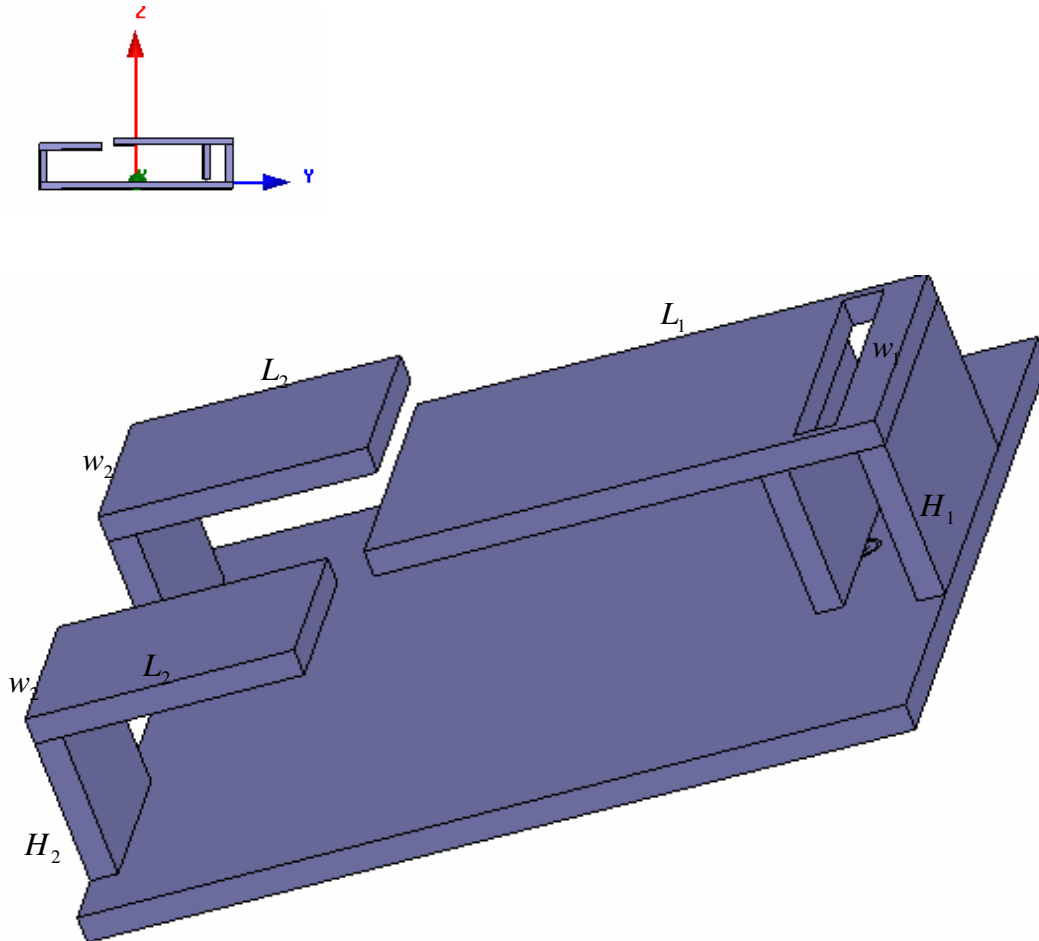


**Figure 18:** The Geometry of PIFDLA.

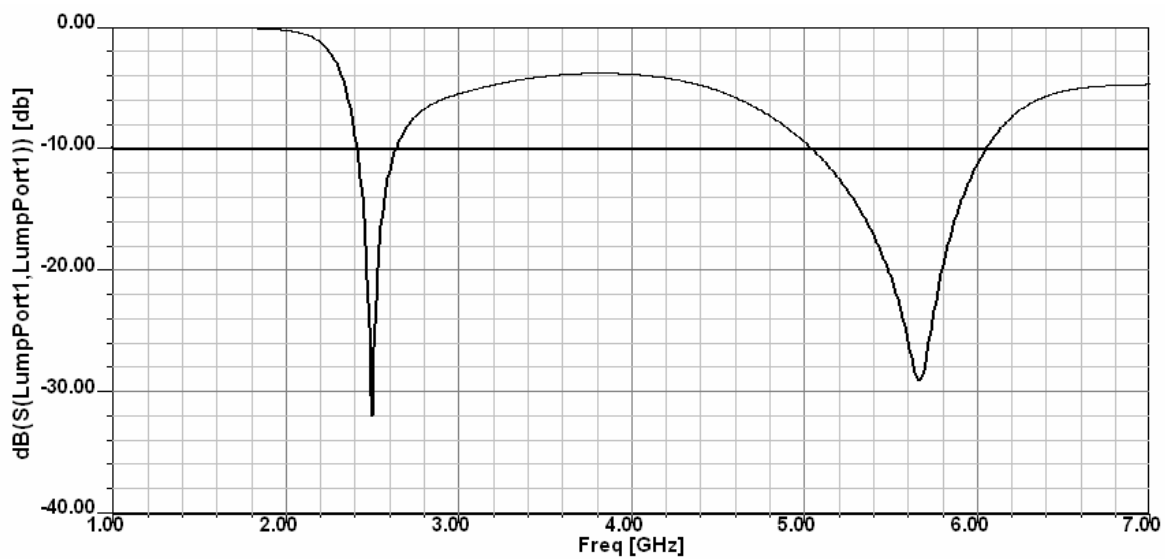
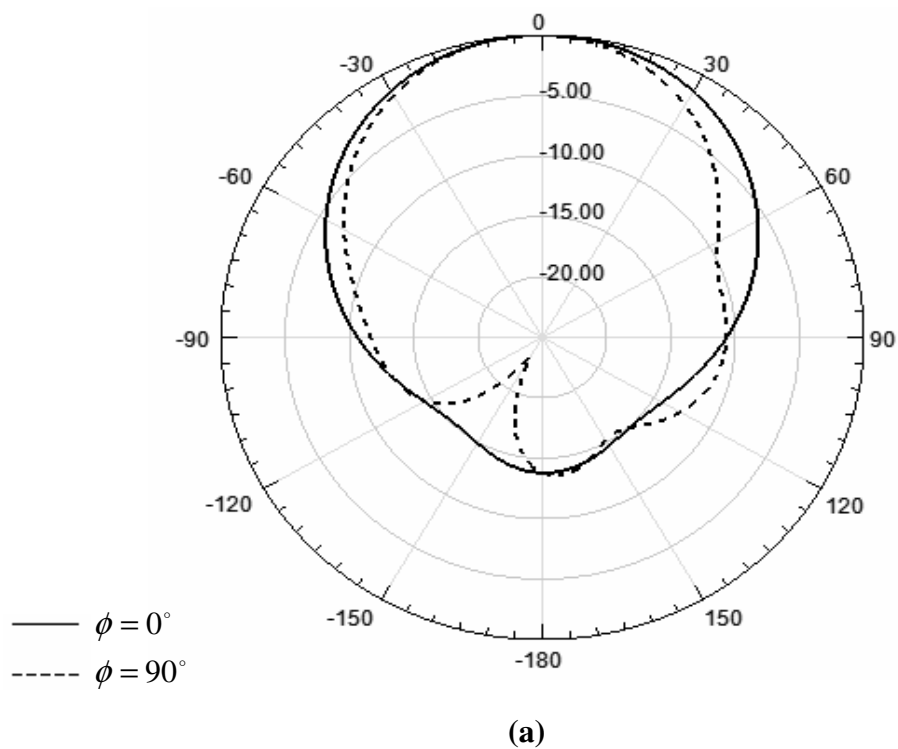
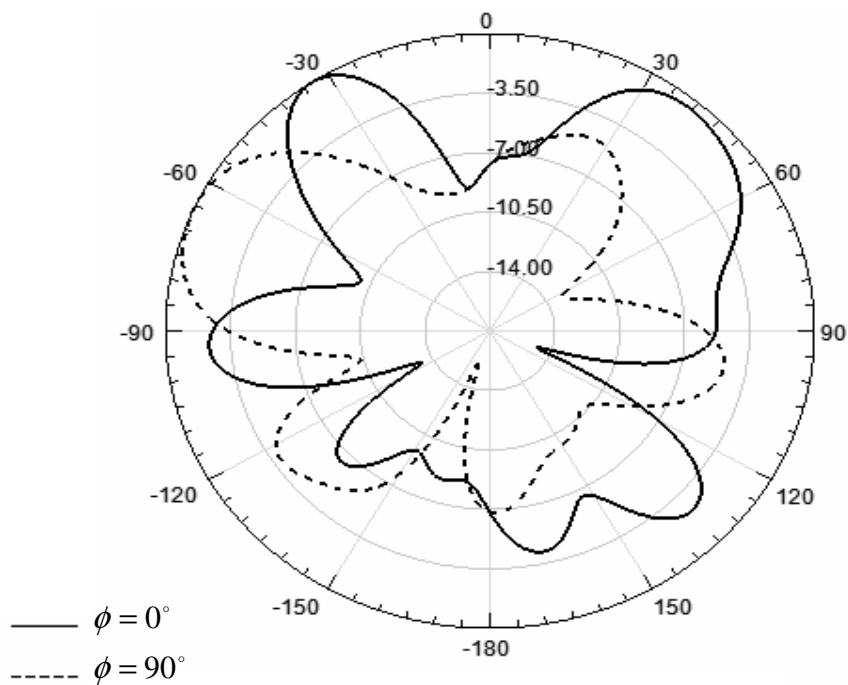


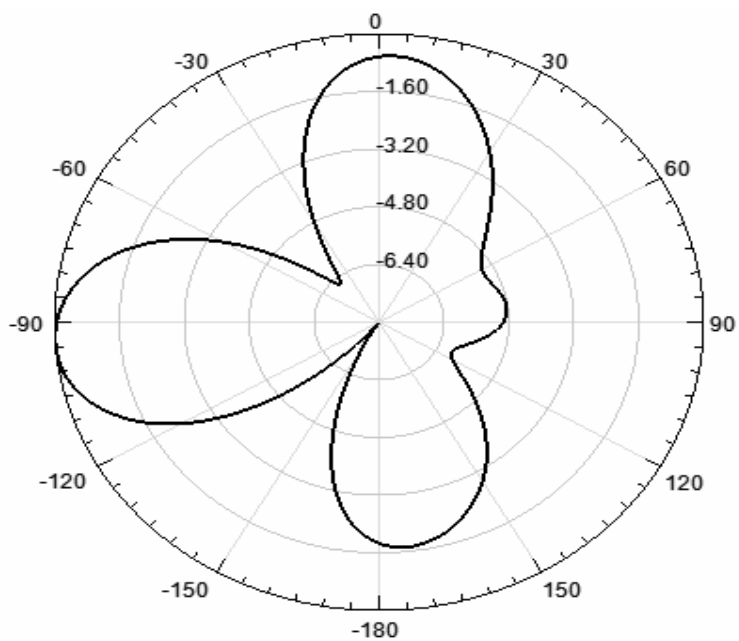
**Figure 19:** The Return Loss for PIFDLA of F-Patch 6 mm above the Ground Plane.



(a)



(b)



(c)

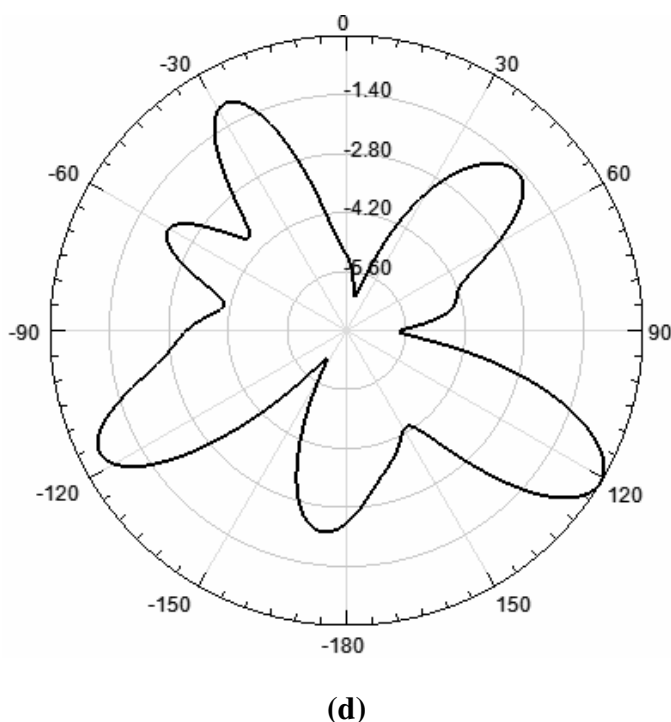


**Figure 20:** The Radiation Pattern for the PIFDLA of F-Patch 6 mm above the Ground Plane (a) with respect to  $\theta$  for  $\phi = 0^\circ$  and  $\phi = 90^\circ$  at 2.5 GHz (b) with respect to  $\theta$  for  $\phi = 0^\circ$  and  $\phi = 90^\circ$  at 5.67 GHz (c) with respect to  $\phi$  for  $\theta = 90^\circ$  at 2.5 GHz (d) with respect to  $\phi$  for  $\theta = 90^\circ$  at 5.67 GHz.

### 3.3.1 The Effect of Short-Circuit Plate Width

To see the effect of the short-circuit plate width  $w_1$ , simulation for different values of short-circuit plate widths (8 mm, 10 mm, and 12 mm) was performed. Results of this simulation are shown in Fig.21, the short-circuit width of  $W < w_1$  (8mm, and 10 mm) gives return loss of -10 dB, and -15 dB, respectively at resonance, so the best result for the lower band was at  $W = w_1 = 12$  mm, because the bandwidth and resonant frequency for PIFA decreases as the short-circuit plate width decreases (Hirisawa, et al., 1992).

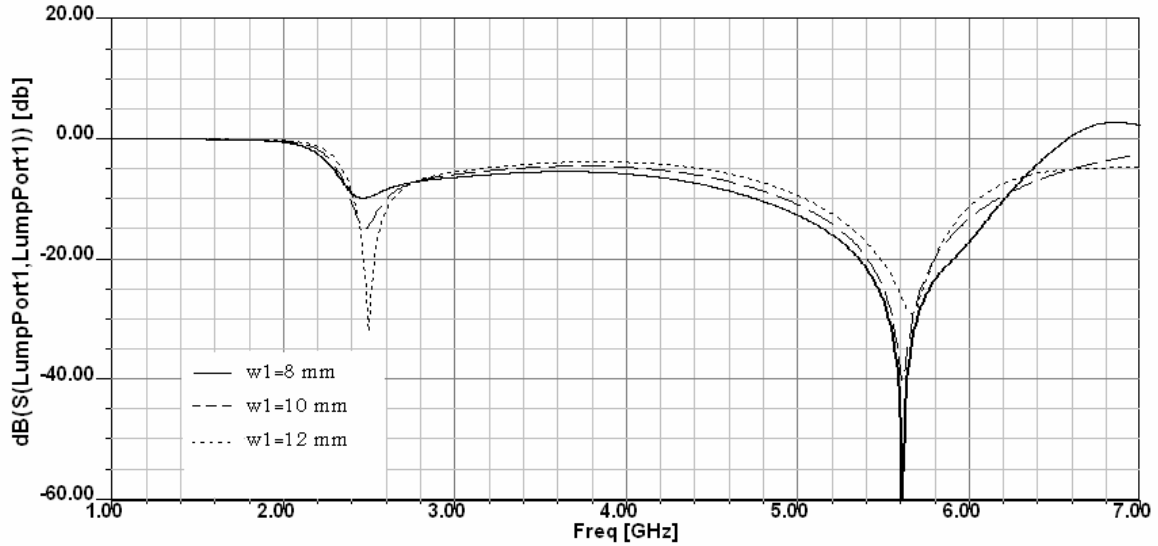


**Figure 21:** The Effect of Short-Circuit Plate Width.

### 3.3.2 The Effect of Finite Ground Plane Size

To see the effect of finite ground plane size (for the idealized case of a ground plane of infinite extent) the antenna may be modeled by using the method of images. For an antenna mounted on a ground plane of finite extent, the outer edge of the ground plane diffracts incident radiation in all directions and consequently currents on the ground plane and antenna differ from those for an infinite ground plane. At the outer edge of the ground plane, the currents on the top and bottom faces of the ground plane are equal in magnitude but opposite in direction because the net current must be zero at the edge. Outer edge diffraction becomes increasingly significant with decreasing size of the ground plane because of increasing magnitude of the currents on the ground plane faces at the outer edge. Edge diffraction can alter the input impedance by more than 100 percent and directive gain in the plane of the ground plane by more than 6 dB from the values for a ground plane of infinite extent (Hirisawa, et al., 1992).

The ground surface waves can produce spurious radiations or couple energy at discontinuities, leading to distortions in the main pattern, or unwanted loss of power. The surface wave effects can be controlled by the use of photonic band gap structures or simply by choosing air as the dielectric. This solves the limitation of poor efficiency as well along with certain degree of bandwidth enhancement.

To see the effect of finite ground plane size on the performance of PIFA, simulations for different sizes of ground plane with length 30 mm to 60 mm of step size 10 mm were performed, these lengths are comparable to  $0.25 \lambda$ ,  $0.3 \lambda$ ,  $0.42 \lambda$ , and  $0.5 \lambda$ . Fig. 22 shows the return loss for square finite ground plane; the lower band is about 350 MHz for ground plane size of 40 mm  $\times$  40 mm, but for ground plane of sizes 50 mm  $\times$  50 mm, and 60 mm  $\times$  60 mm, the return loss is -10 dB, -14 dB respectively.

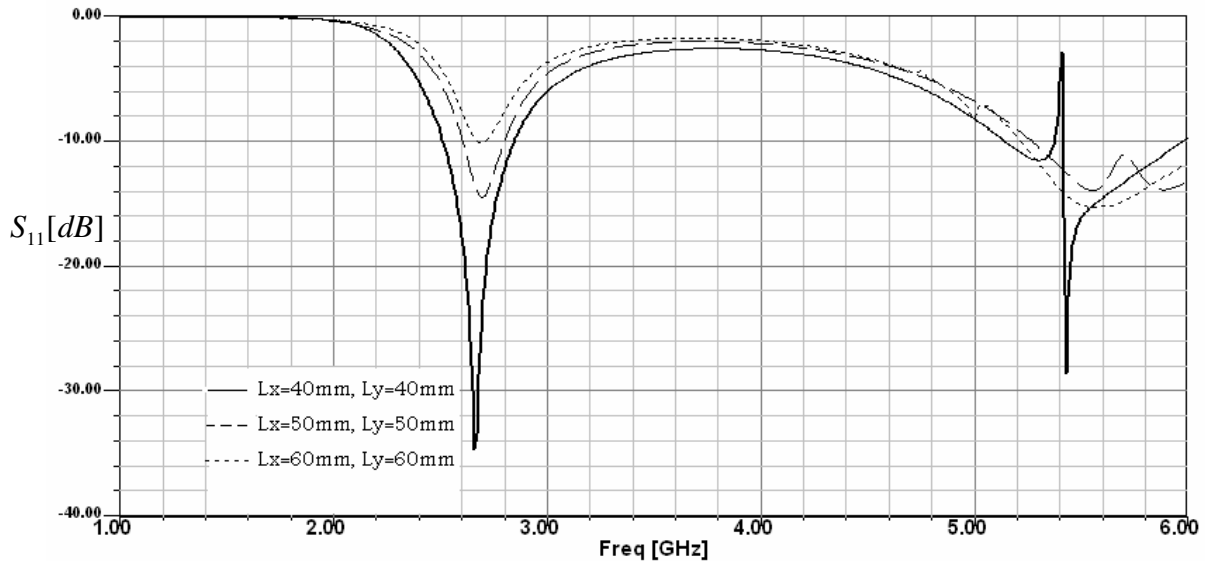


**Figure 22:** The Effect of Square Finite Ground Plane on PIFA

The return loss for rectangular ground plane with length  $0.25 \lambda$  in x-axis and  $0.3 \lambda$ ,  $0.42 \lambda$ , and  $0.5 \lambda$  in y-axis is shown in Fig.23. For ground plane of size  $30 \text{ mm} \times 40 \text{ mm}$ , the return loss for the lower band is  $-13.5 \text{ dB}$ . For ground plane of size  $30 \text{ mm} \times 50 \text{ mm}$ ,  $30 \text{ mm} \times 60 \text{ mm}$  the lower band is  $300 \text{ MHz}$ , and  $260 \text{ MHz}$  respectively starting at  $2.6 \text{ GHz}$  instead of  $2.4 \text{ GHz}$  for ground plane of size  $30 \text{ mm} \times 30 \text{ mm}$ .

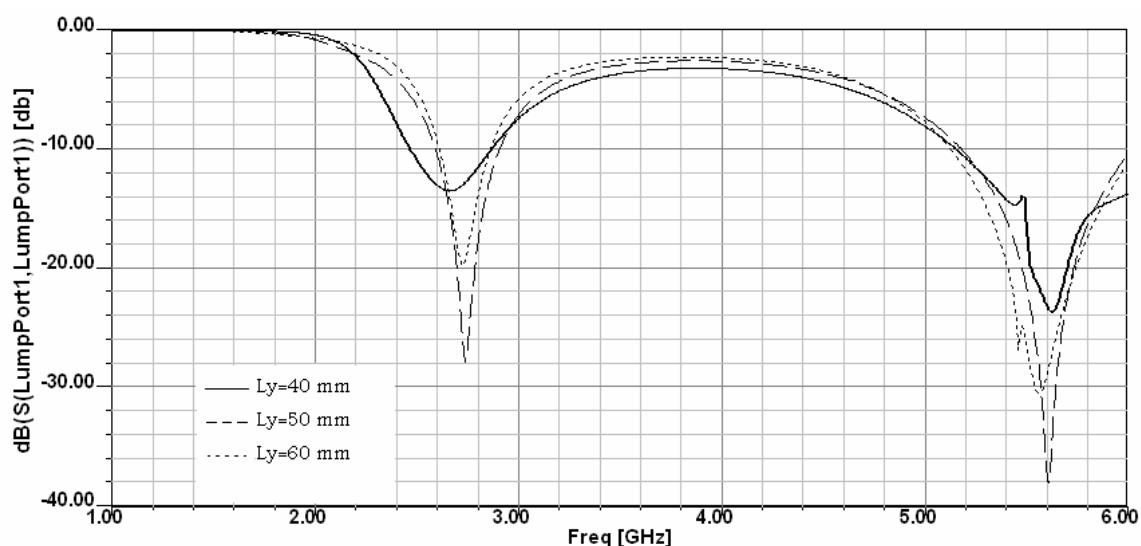


**Figure 23:** The Return Loss of PIFA for Rectangular Ground Plane with  $0.25 \lambda$  length in x-axis.

The return loss for rectangular ground plane with length  $0.25 \lambda$  in y-axis and  $0.3 \lambda$ ,  $0.42 \lambda$ , and  $0.5 \lambda$  in x-axis is shown in Fig.24. For ground plane of size  $50 \text{ mm} \times 30 \text{ mm}$ ,  $60 \text{ mm} \times 30 \text{ mm}$ , the return loss for the lower band is  $-12 \text{ dB}$ , and  $-15 \text{ dB}$  respectively. For ground plane of size  $40 \text{ mm} \times 30 \text{ mm}$ , the lower band is  $240 \text{ MHz}$  starts at  $2.46 \text{ GHz}$ , and the upper band is  $600 \text{ MHz}$  with return loss  $-15.5 \text{ dB}$ . As a result, the best size of ground plane for our antenna design was to be a square ground plane with length of  $0.25 \lambda$ . Also it

is worthwhile to know that the simulation and measurement results show that the resonant frequency and bandwidth of the PIFA oscillate as the ground plane size increases and converges to the values for the PIFA mounted on an infinite ground plane (Hirisawa, et al., 1992).

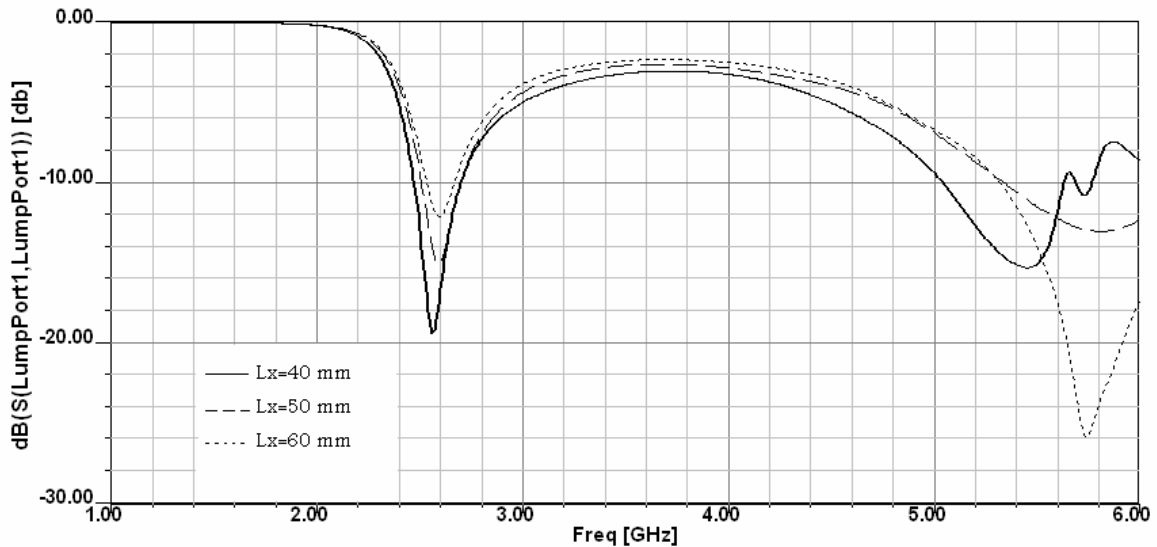


**Figure 24:** The Return Loss of PIFA for Rectangular Ground Plane with  $0.25 \lambda$  length in y-axis.

The position of a PIFA on a finite ground plane is considered; the characteristic of PIFAs mounted at different locations on a ground plane and with different orientations was studied, the feed location was adjusted so that the antenna is matched to  $50 \Omega$  at resonance. From those results, it was found that the PIFA should be placed close to the corner of the ground plane where the short-circuit plate is at the ground plane edge for optimal gain and performance (Hirisawa, et al., 1992).



### 3.3.3 The Effect of Coaxial Cable Length

Also the effect of coaxial cable length is considered, a simulation for different coaxial cable lengths from 1 mm to 5 mm with 1 mm step size was performed. Fig.25 shows the return loss for different coaxial cable lengths, in which the coaxial cable length does not affect the bandwidth for the upper and lower bands, but causes small shift in the resonant frequency for the upper band.

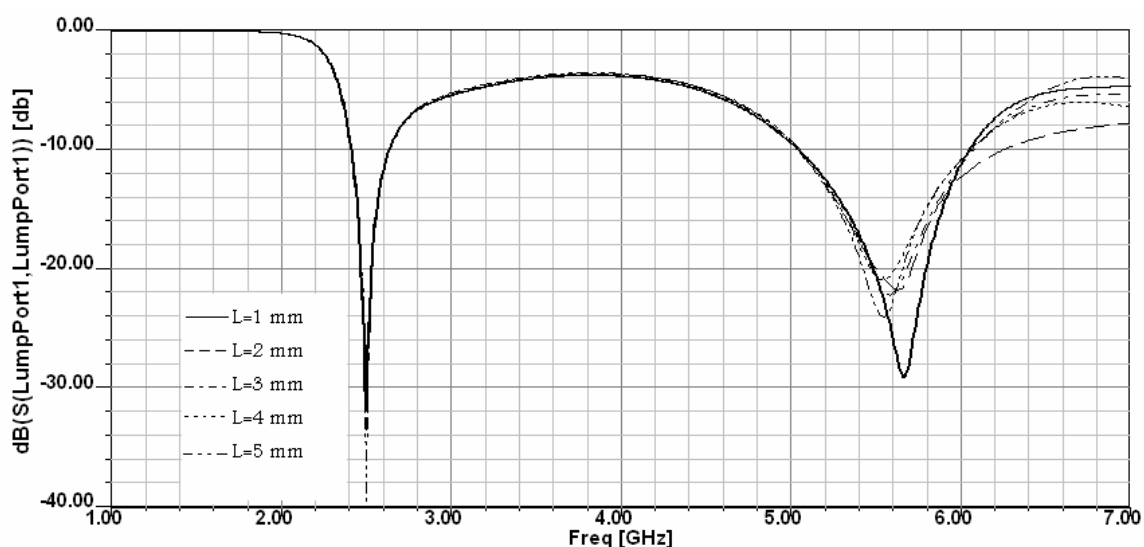
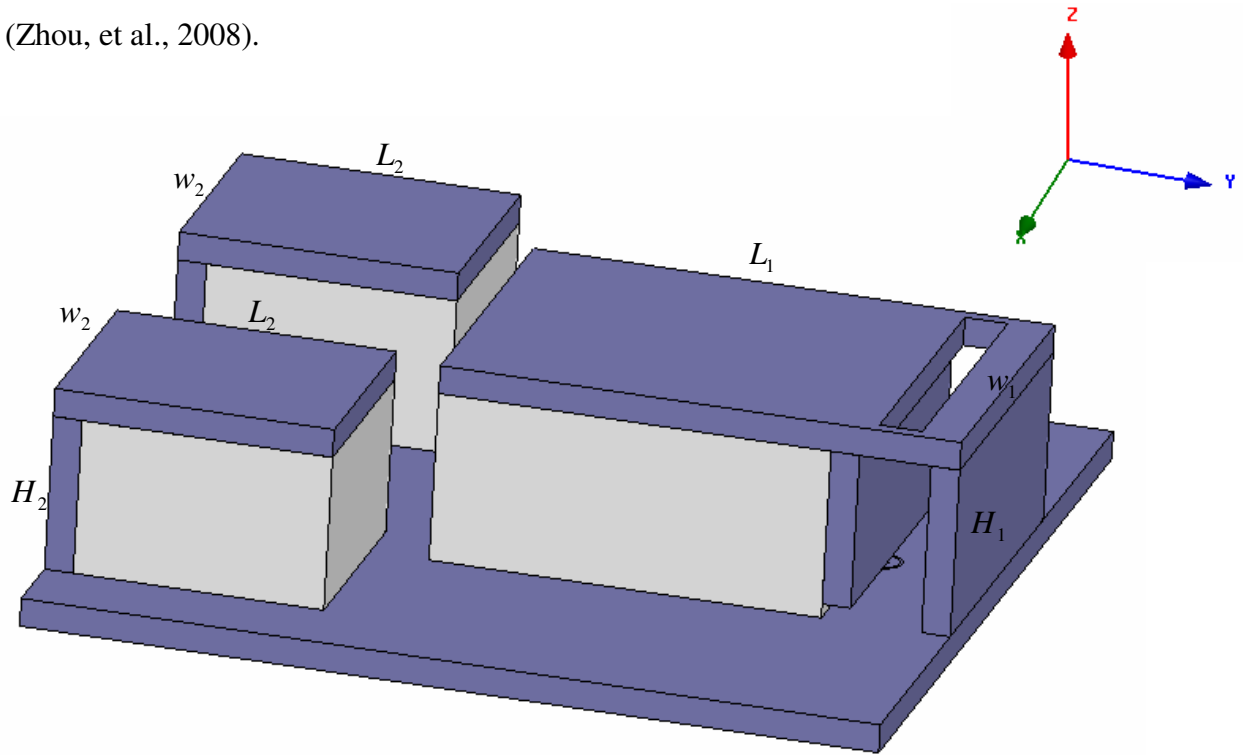


**Figure 25:** The Return Loss for Different Coaxial Cable Lengths.

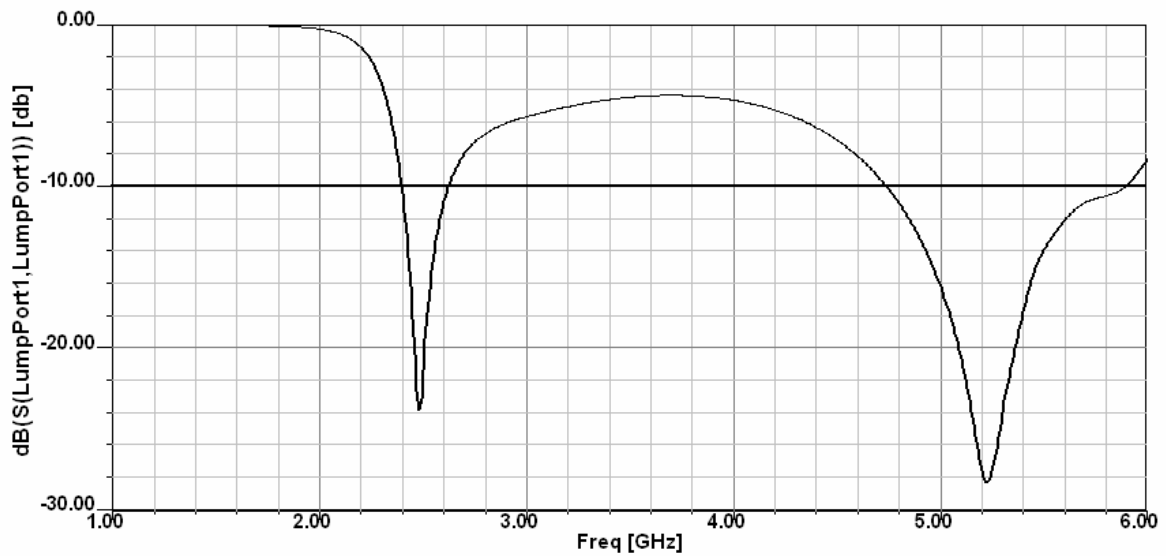
### 3.3.4 The Effect of Substrate

For PIFDLA - F-patch 6mm from the ground plane- to support the upper plates, substrate of dielectric material ( $\epsilon_r = 1.2$ ) is added as in Fig.26. By adjusting all antenna parameters ( $L_1 = 18.2$  mm,  $w_1 = 12$  mm,  $H_1 = 7$  mm,  $L_2 = 9.75$  mm,  $w_2 = 8$  mm,  $H_2 = 6.5$  mm), Figs.27 and 28 show the return loss and radiation pattern respectively for supported antenna. Fig.27 shows an enhancement of 15% on the lower band (2.39 GHz-2.62 GHz)

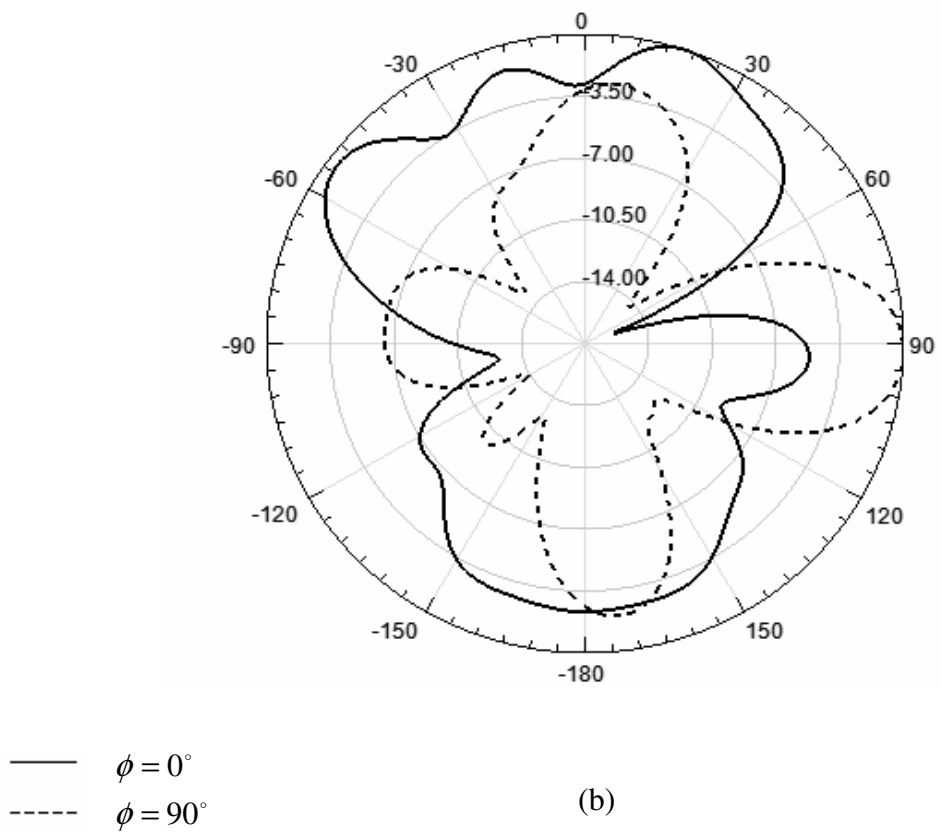
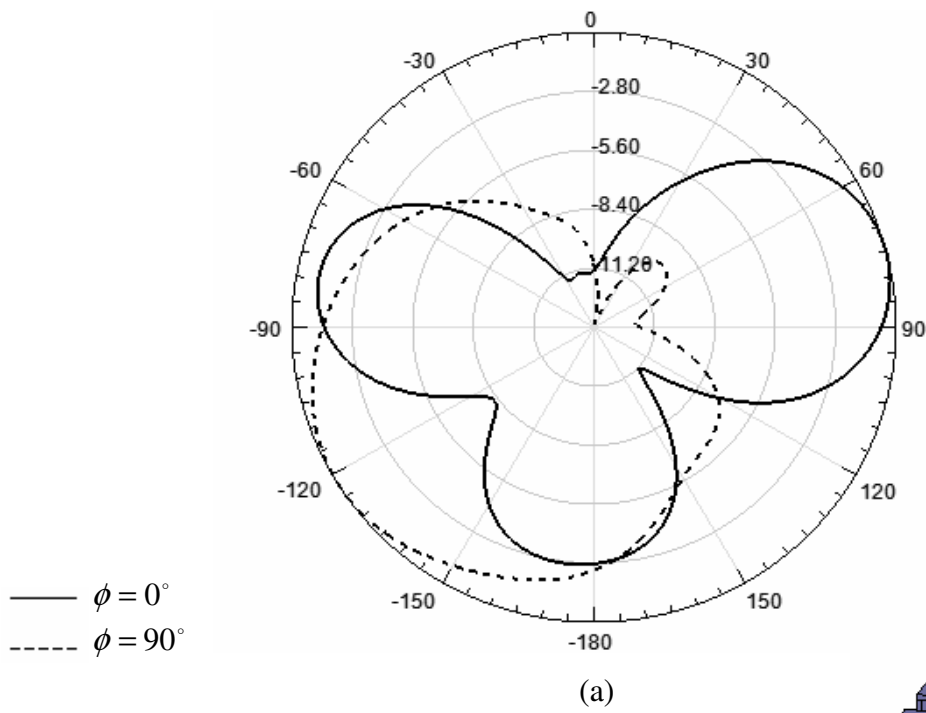
and 78.5% on the upper band (4.74 GHz-5.9 GHz) with gain 7.6 dB, 7.3 dB at 2.48 GHz and 5.22 GHz respectively, in addition to size reduction of 12.5% compared with PIFLA of (Zhou, et al., 2008).

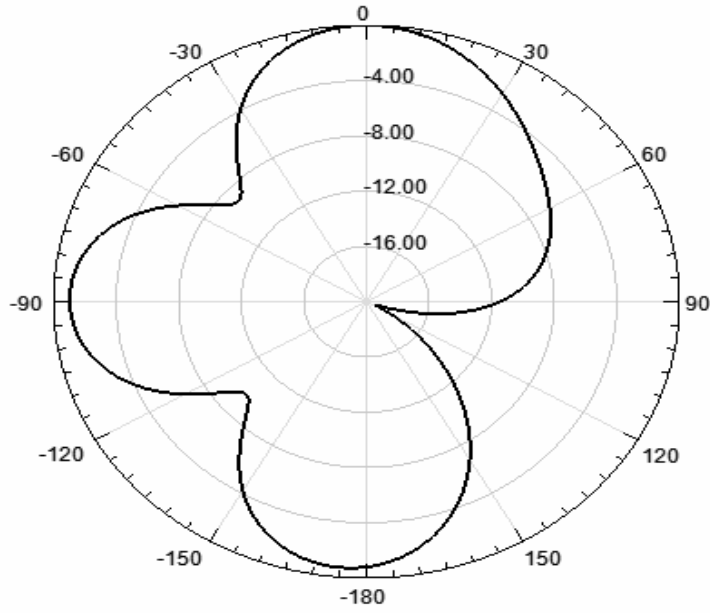


**Figure 26:** The Geometry of PIFDLA supported by Substrate.

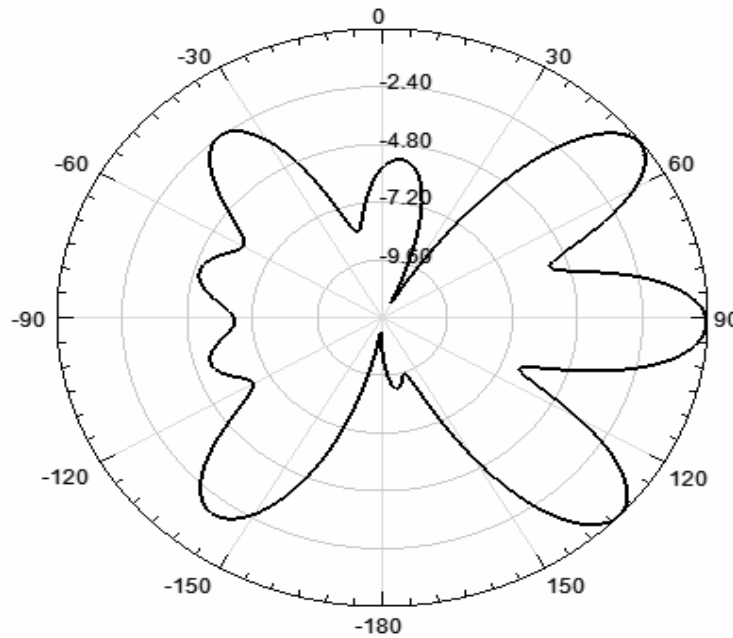


**Figure 27:** The return Loss for PIFDLA with dielectric material as Substrate ( $\epsilon_r = 1.2$ )





(c)



(d)

**Figure 28:** The Radiation Pattern of PIFDLA with  $\epsilon_r=1.2$  Substrate (a) with respect to  $\theta$  for  $\phi=0^\circ$  and  $\phi=90^\circ$  at 2.48 GHz (b) with respect to  $\theta$  for  $\phi=0^\circ$  and  $\phi=90^\circ$  at 5.22 GHz (c) with respect to  $\phi$  for  $\theta=90^\circ$  at 2.48 GHz (d) with respect to  $\phi$  for  $\theta=90^\circ$  at 5.22 GHz.

good results obtained by supporting the antenna with dielectric material  $\epsilon_r = 1.2$ , lead us to start with the PIFDLA antenna with substrate that covers all the ground plane with  $\epsilon_r = 1.2$  and height of 7 mm for inverted-F which is 7 mm above the ground plane and 4.5 mm for inverted-L which is 4.5 mm above the ground plane, in addition to the copper thickness of 1 mm for copper conductors and removing the slot between the feeding plate and short-circuit plate. By adjusting all parameters ( $L_1 = 18.4$  mm,  $w_1 = 12$  mm,  $H_1 = 8$  mm,  $L_2 = 9.5$  mm,  $w_2 = 8.5$  mm,  $H_2 = 5.5$  mm), this proposed antenna operates from 2.37GHz to 2.55GHz for the lower band and from 5.01GHz to 5.72GHz for the upper band. But for the copper thickness of 0.17mm for F-patch and L-patches and copper thickness of 1 mm for short-circuit plates with substrate of height 7.5mm for the inverted-F antenna and 6mm for the inverted-L antenna; the antenna operates from 2.36 GHz to 2.56 GHz for the lower band and from 4.88 GHz to 5.69 GHz for the upper band. Figs. 29, 30 and 31 show the geometry return loss and radiation pattern respectively for supported antenna of copper thickness 0.17 mm.

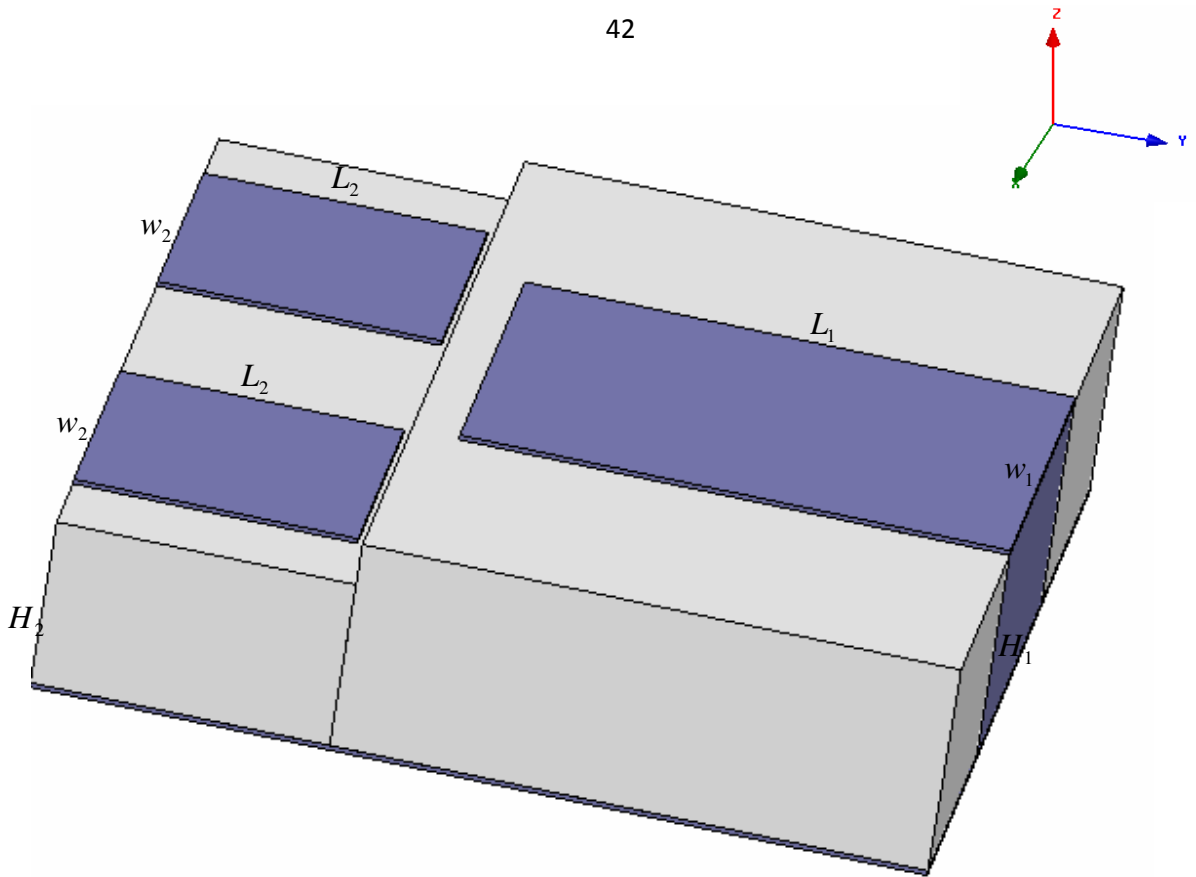


**Figure 29:** The Geometry of supported PIFDL Antenna with Copper Thickness 0.17 mm.

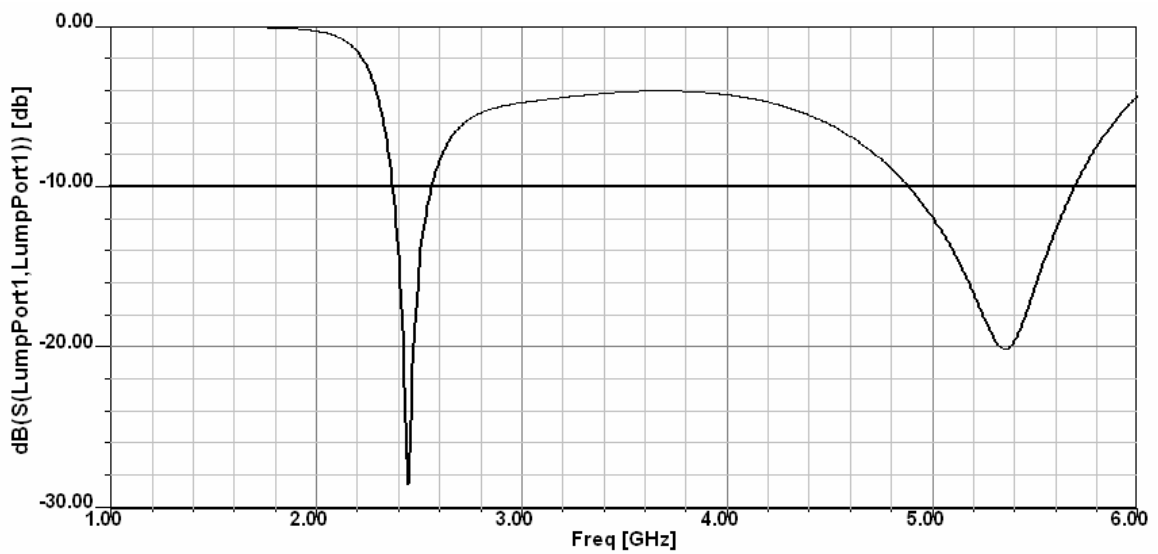
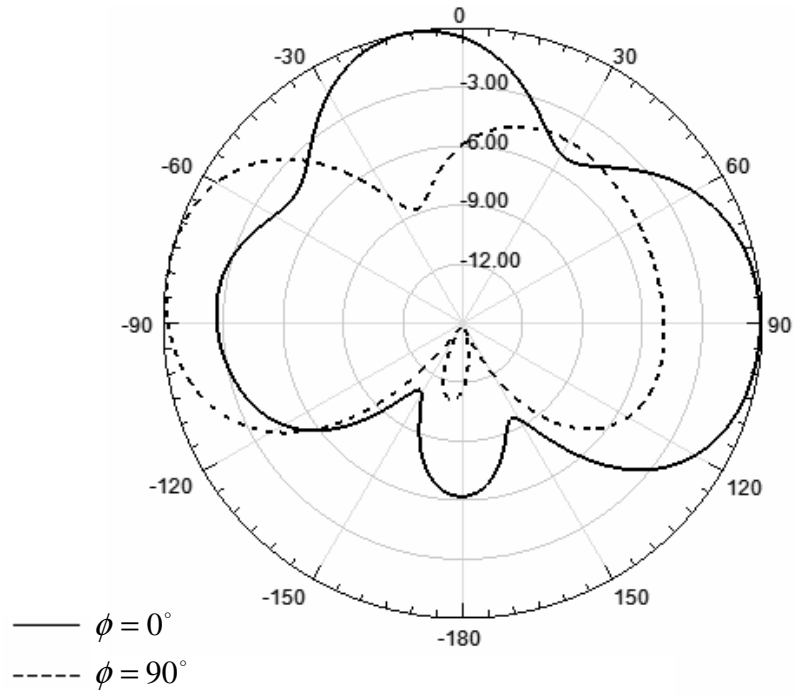
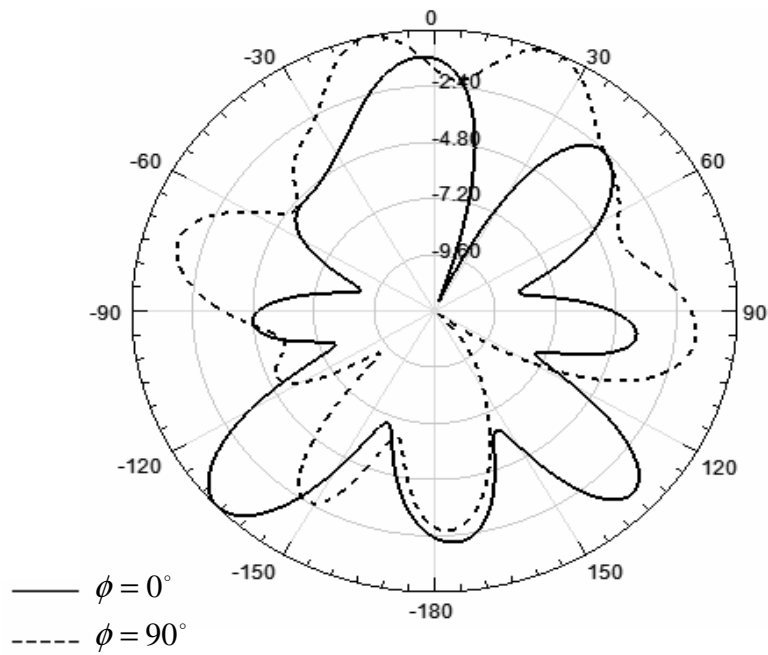
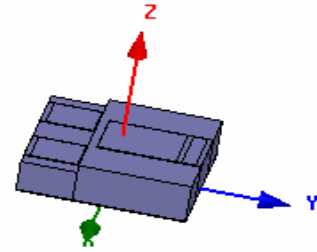


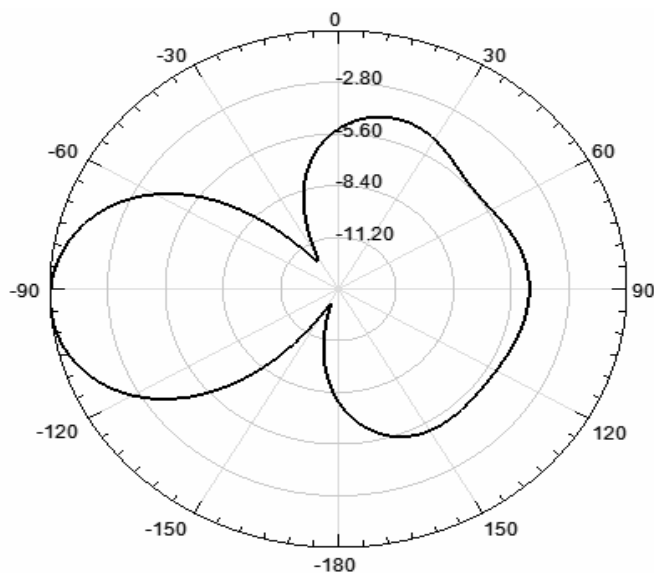
**Figure 30:** The Return loss for supported PIFDL Antenna with 0.17 mm Copper Thickness.



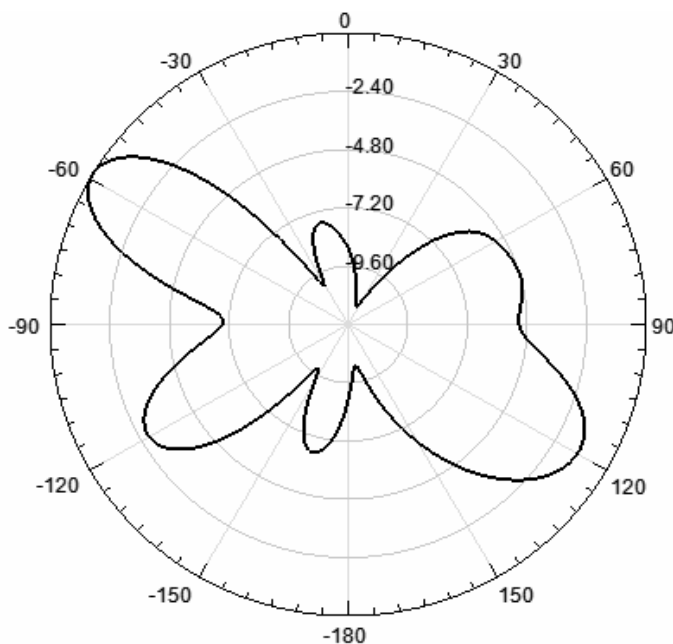
(a)



(b)



(c)



(d)

**Figure 31:** The Radiation Pattern for supported PIFDL antenna with 0.17 mm copper thickness (a) with respect to  $\theta$  for  $\phi = 0^\circ$  and  $\phi = 90^\circ$  at 2.45 GHz (b) with respect to  $\theta$  for  $\phi = 0^\circ$  and  $\phi = 90^\circ$  at 5.35 GHz (c) with respect to  $\phi$  for  $\theta = 90^\circ$  at 2.45 GHz (d) with respect to  $\phi$  for  $\theta = 90^\circ$  at 5.35 GHz.



### 3.3.5 Measurement Results

We measured the return loss and voltage standing wave ratio (VSWR) for the PIFDLA of Fig.18 using network analyzer with frequency range up to 3 GHz, so only the lower band appears. Figs. 32, 33 show the return loss and VSWR respectively for PIFDLA of Fig.18. From Fig.32, the lower band is from 2.37 GHz to 2.59 GHz at resonance of 2.48 GHz, but for PIFDLA of Fig.18 the lower band is from 2.4 GHz to 2.63 GHz at resonance of 2.5 GHz which means that there is about 20 MHz frequency shift at resonance between simulated and measured results, and this due to inaccurate dimensions for measured PIFDLA compared with the dimensions of simulated one.

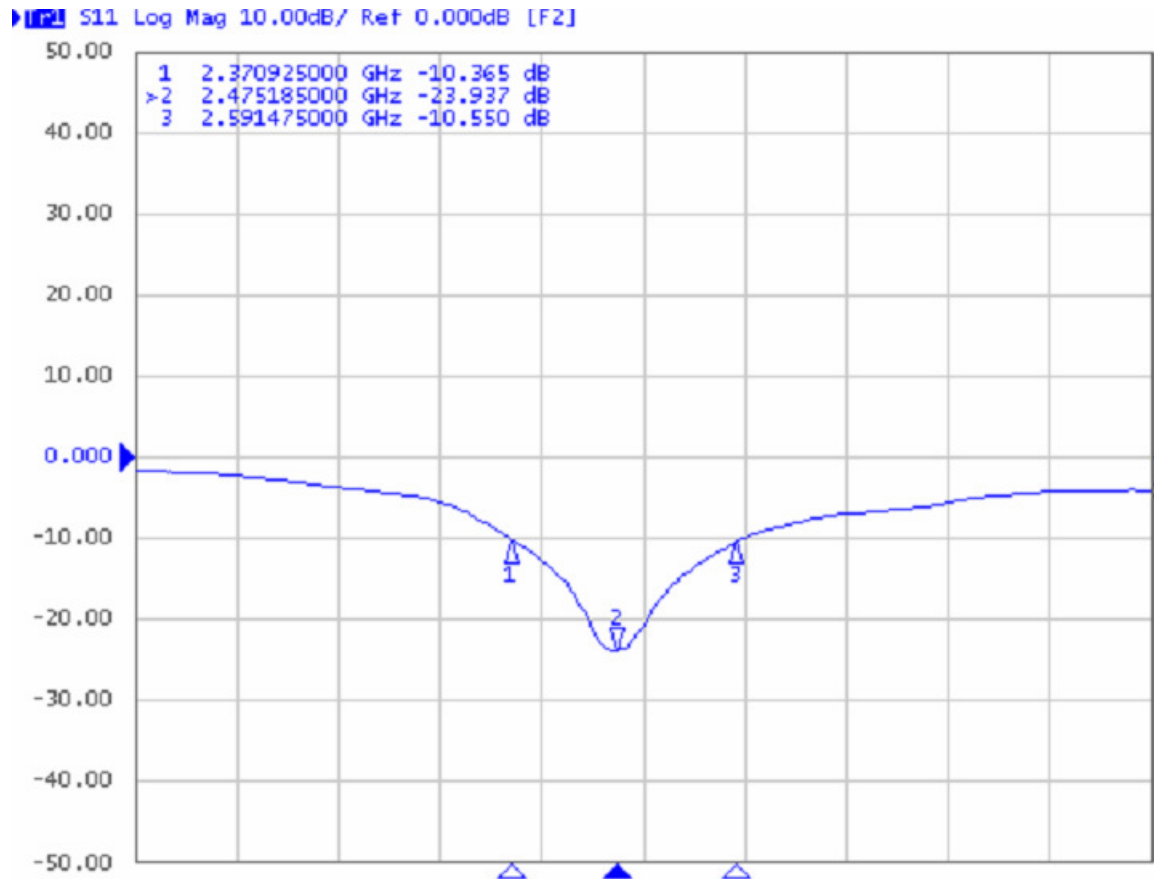


**Figure 32:** The Measured Return Loss for PIFDLA of Fig.18

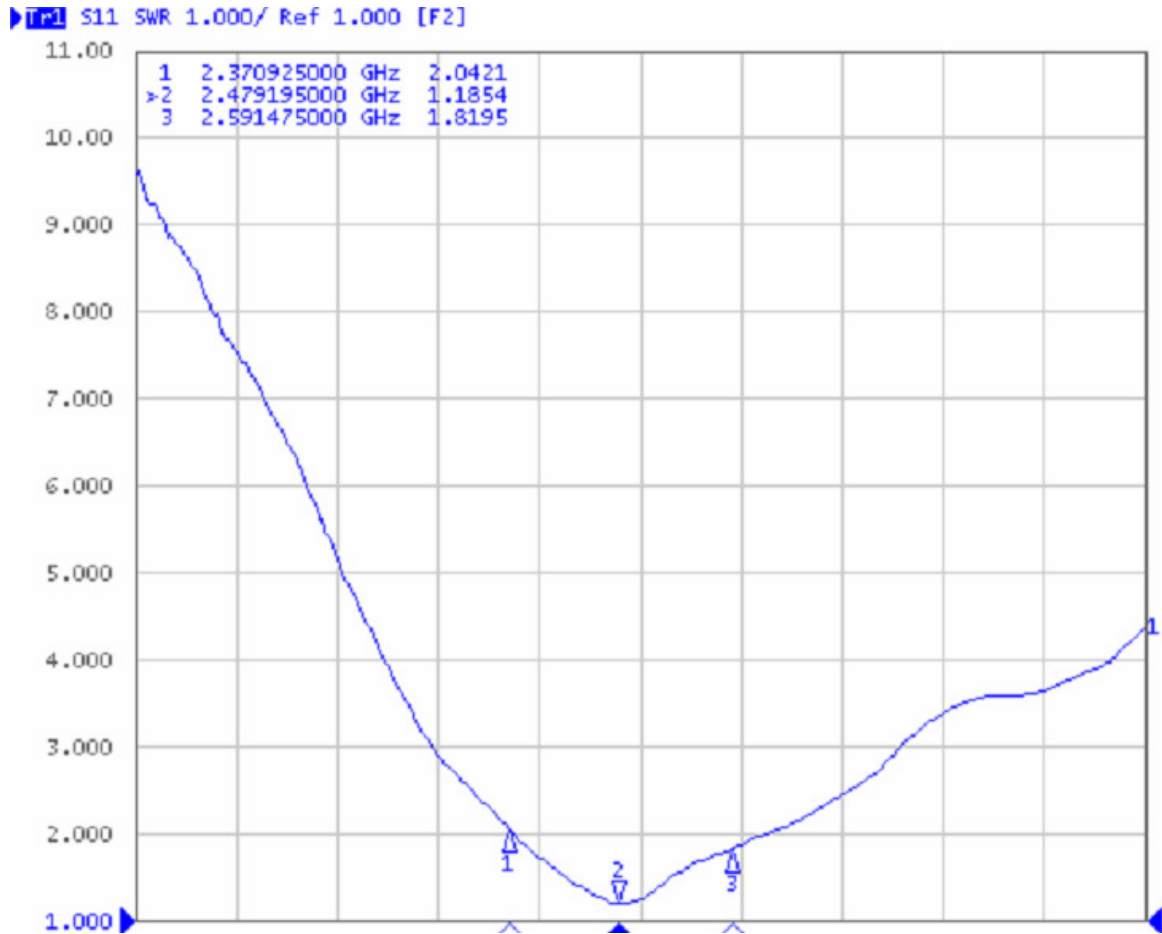
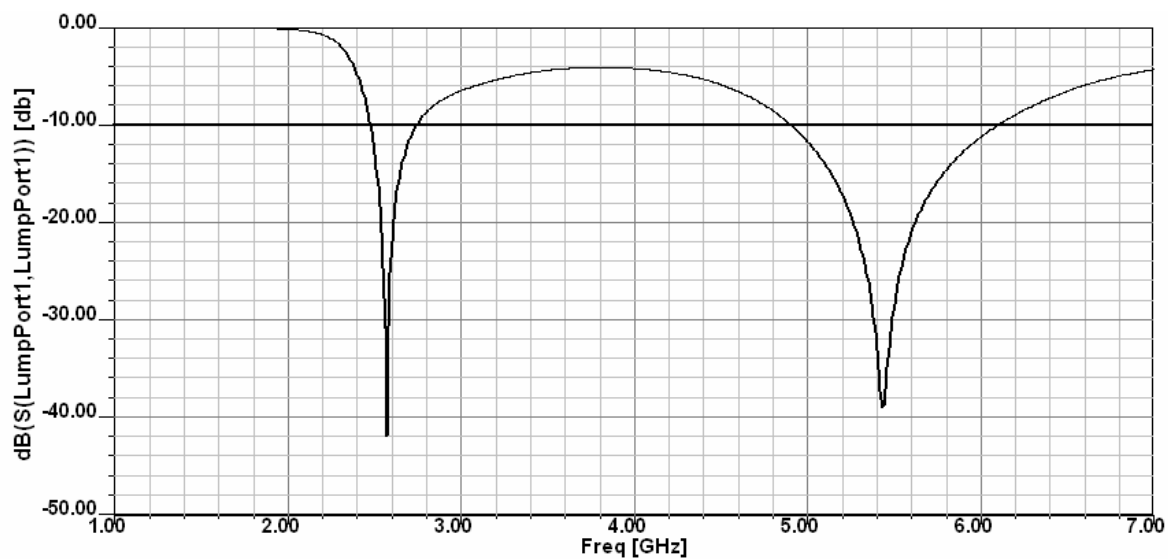


**Figure 33:** The VSWR of PIFDLA of Fig.18

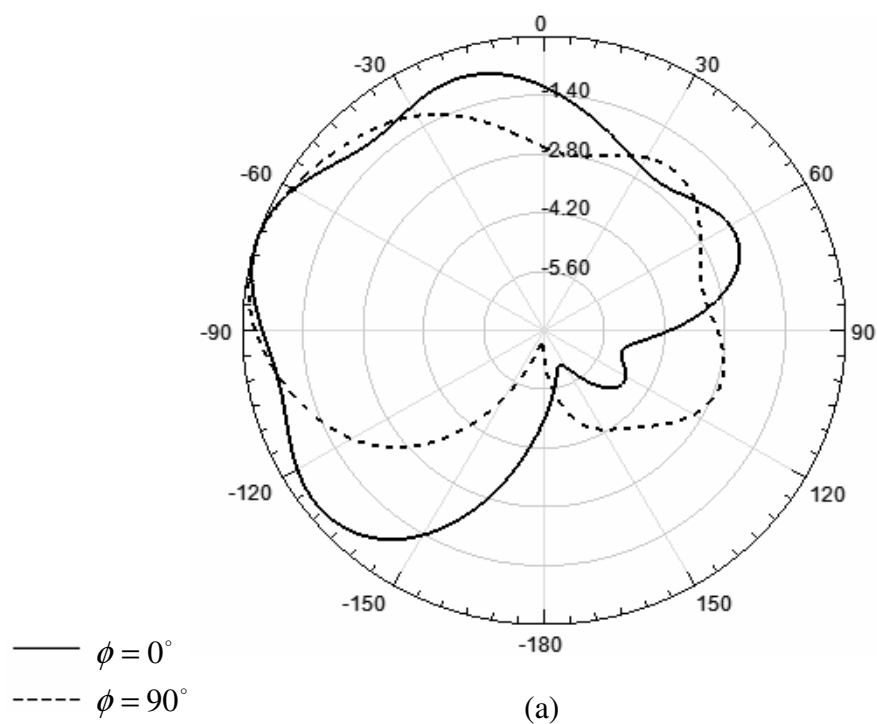
### 3.4 Multiband PIFDLA for WLAN Applications and WiMAX

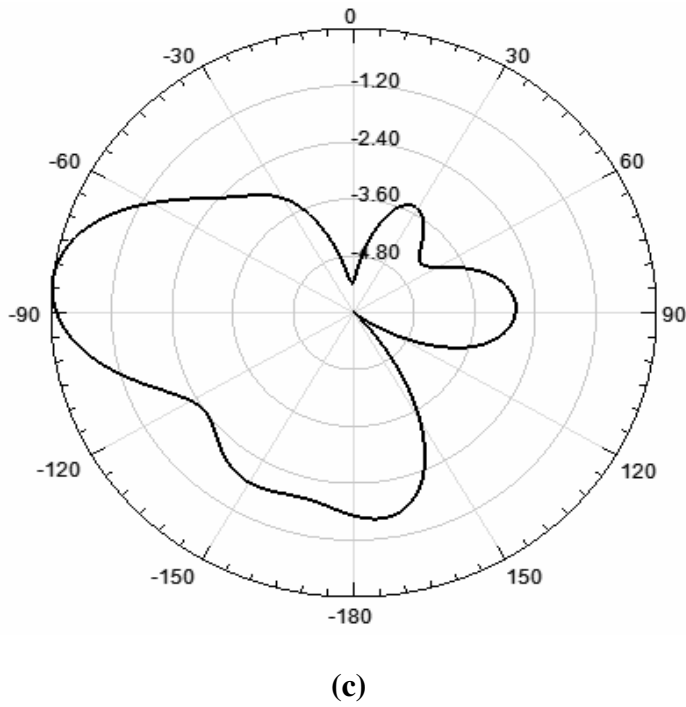
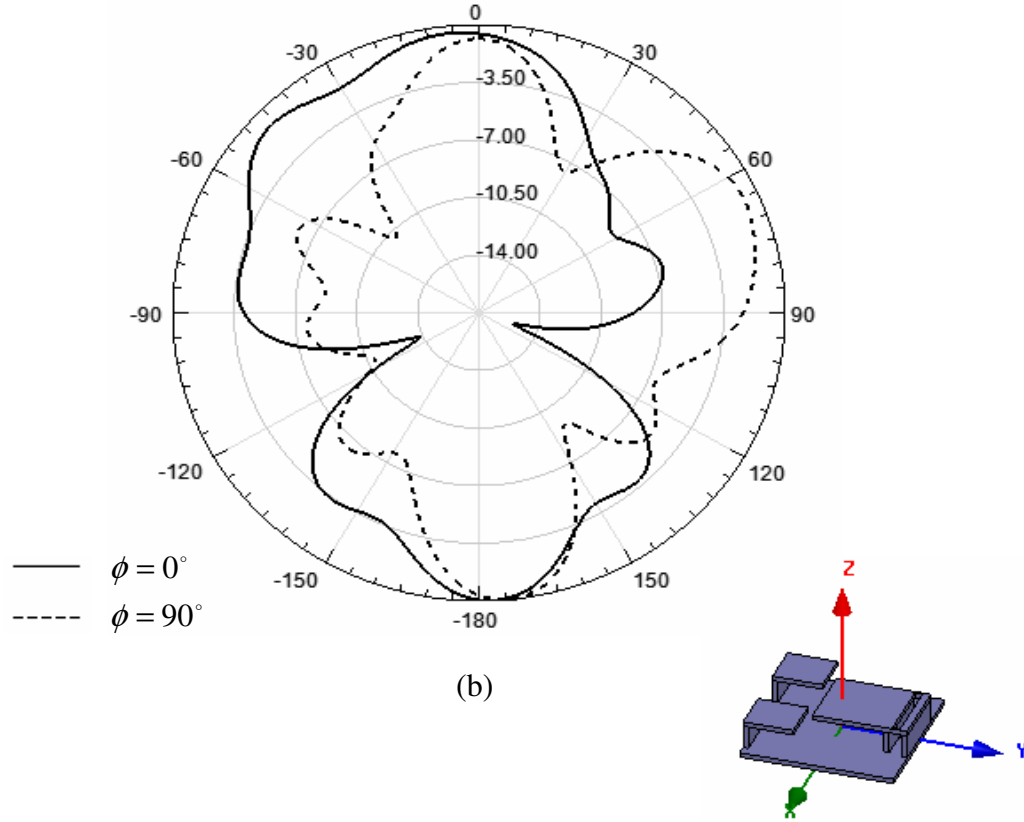
By the same way as in section 3.3 but with 5 mm between the F-patch and the ground plane instead of 6mm and with air substrate, the lower band enhanced by 35% (2.47 GHz-2.74 GHz) and the upper band enhanced by 84.6% (4.9 GHz-6.1 GHz) in addition to size reduction of 25% and gain 7.8 dB and 6.5 dB at 2.57 GHz and 5.44 GHz respectively compared with PIFA of (Zhou, et al., 2008). This proposed multiband single-feed PIFA simultaneously operates in the IEEE 802.11a/b/g, HIPERLAN2 and WiMAX band (2.5GHz-2.7GHz) instead of Bluetooth (2.4 GHz-2.48 GHz). Figs.34 and 35 show the

return loss and radiation pattern respectively of this Planar Inverted-F Dual-L Antenna (PIFDLA).



**Figure34:** The Return Loss for PIFDLA of F-Patch 5mm above the Ground Plane.





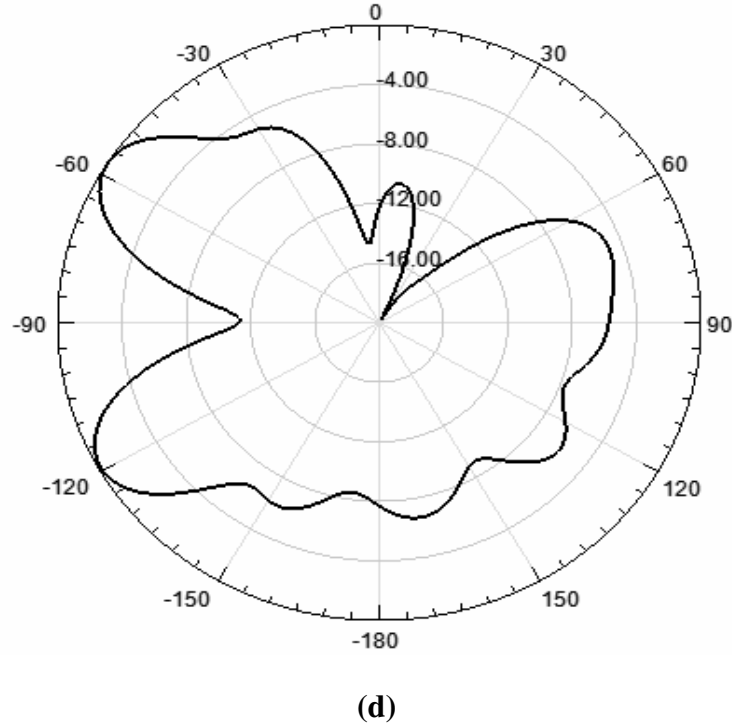


**Figure 35:** The Radiation Pattern for PIFDLA of F-Patch 5mm above the Ground Plane (a) with respect to  $\theta$  for  $\phi = 0^\circ$  and  $\phi = 90^\circ$  at 2.57 GHz (b) with respect to  $\theta$  for  $\phi = 0^\circ$  and  $\phi = 90^\circ$  at 5.44 GHz (c) with respect to  $\phi$  for  $\theta = 90^\circ$  at 2.57 GHz (d) with respect to  $\phi$  for  $\theta = 90^\circ$  at 5.44 GHz.

By the same way we supported the PIFDLA – 5 mm F-patch above the ground plane –by dielectric material  $\epsilon_r = 1.2$ , the return loss and radiation pattern for this antenna with ( $L_1 = 18.4$  mm,  $w_1 = 14$  mm,  $H_1 = 6.1$  mm,  $L_2 = 9.75$  mm,  $w_2 = 8.75$  mm,  $H_2 = 5.9$  mm) are shown in Figs.36,37, respectively. Fig.34 shows an enhancement of 10% on the lower band (2.41 GHz-2.63 GHz) and an enhancement of 81.5% on the upper band (4.68GHz-5.86 GHz) with gain 7.48 dB, 7.2 dB at 2.5 GHz and 5.19 GHz respectively in addition to size reduction of 24% compared to PIFLA of (Zhou, et al., 2008). Note that the existent of substrate shifts the lower frequency band to operate on Bluetooth instead of WiMAX band.

Note: Table 1 shows a summary of final results for different modifications on PIFLA compared with (Zhou, et al., 2008).

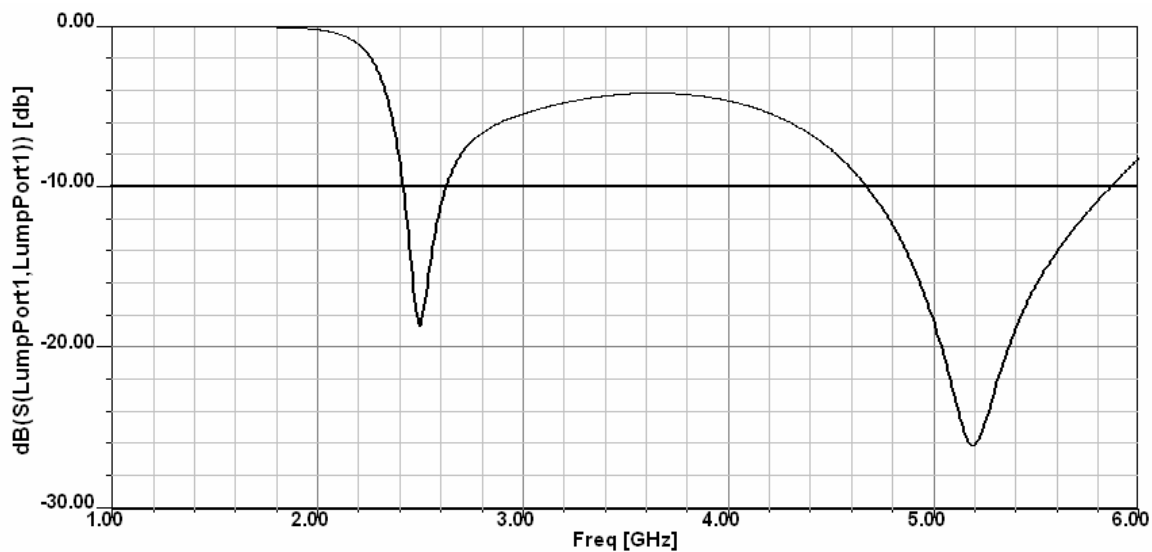
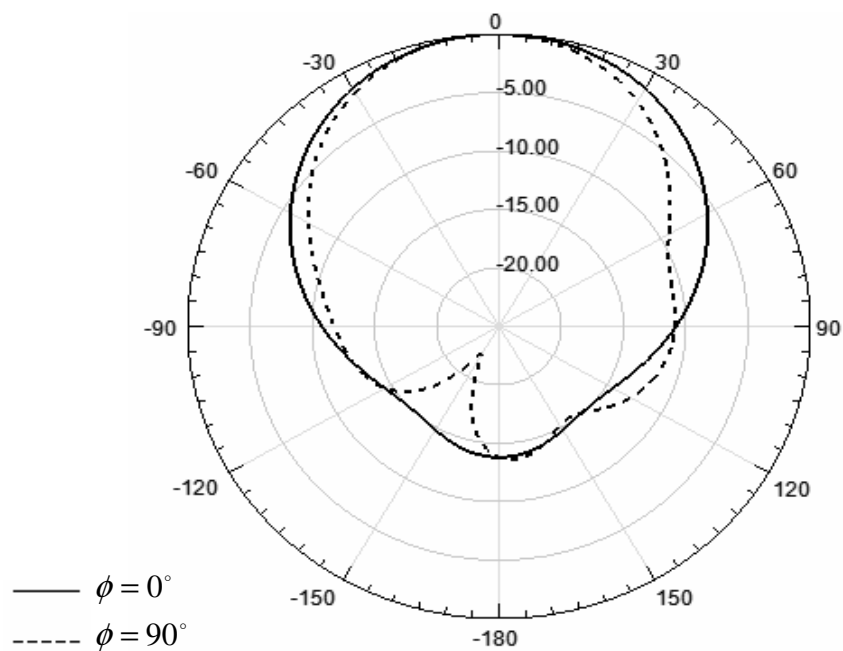
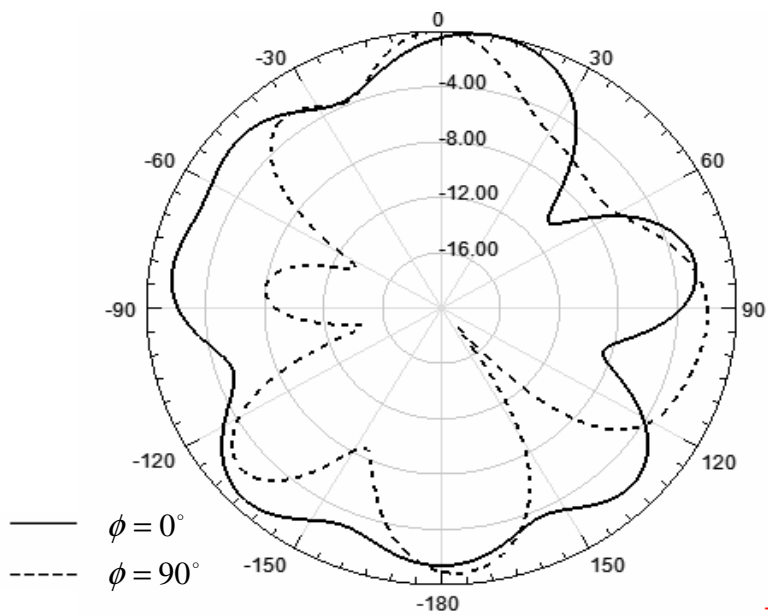


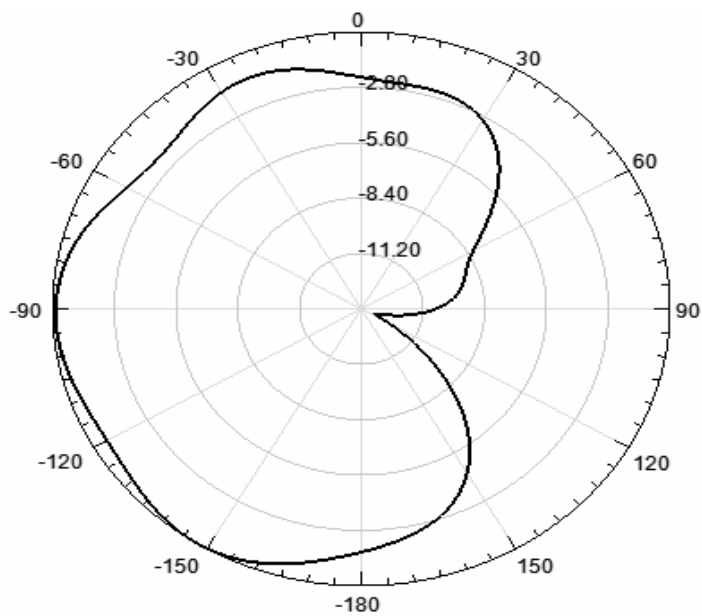
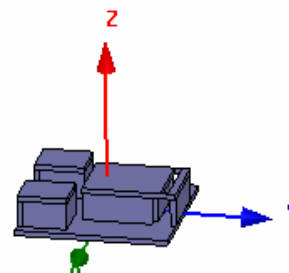
**Figure 36:** The Return Loss for PIFDLA of F-patch 5mm above the ground plane with Substrate  $\epsilon_r=1.2$



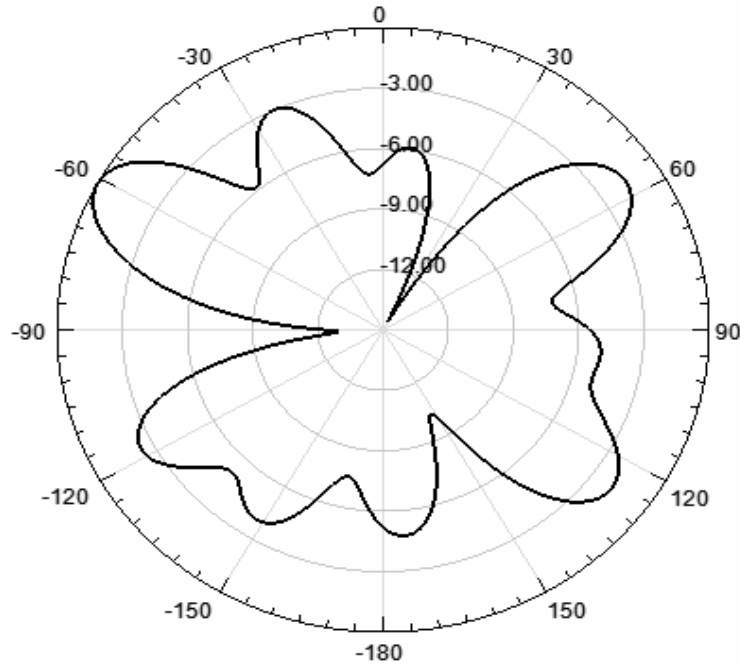
(a)



(b)



(c)



(d)

**Figure 37:** The Radiation Pattern for PIFDLA of F-patch 5mm above the ground plane with Substrate (a) with respect to  $\theta$  for  $\phi = 0^\circ$  and  $\phi = 90^\circ$  at 2.5 GHz (b) with respect to  $\theta$  for  $\phi = 0^\circ$  and  $\phi = 90^\circ$  at 5.19 GHz (c) with respect to  $\phi$  for  $\theta = 90^\circ$  at 2.5 GHz (d) with respect to  $\phi$  for  $\theta = 90^\circ$  at 5.19 GHz.



**Table 1:** Summary of Final Results

	Bandwidth of the Lower band	Bandwidth of the Upper band	Bandwidth enhancement for the		Size reduction (%)
			Lower band (%)	Upper band (%)	
PIFLA(Zhou, et al., 2008)	200 MHz	650 MHz	Our reference		Our reference
PIFDLA of F-patch 6mm above the ground plane	230 MHz	1000 MHz	15%	53.8%	12.5%
Supported PIFDLA of F-patch 6mm above the ground plane	230 MHz	1160 MHz	15%	78.5%	12.5%
Supported PIFDLA with 0.17 mm copper thickness	200 MHz	810 MHz	0%	24.6%	4%
PIFDLA of F-patch 5mm above the ground plane	270 MHz	1200 MHz	35%	84.6%	25%
Supported PIFDLA of F-patch 5 mm above the ground plane	220 MHz	1180 MHz	10%	81.5%	24%

## CHAPTER FOUR

### CONCLUSIONS AND RECOMMENDATIONS FOR FUTURE WORK

The rapid growth of local area network (WLAN) applications has created strong demands for small internal antennas. Due to the limited space availability in the wireless devices, the design of low cost and small size antennas is required. In current wireless environments, there are many wireless devices working in several frequency bands, and providing different services. There is an increasing need to provide many of such wireless services with one device. However, this normally requires many antennas to cover each service, and it is not possible to fit them all in a small device. To address this requirement, antennas that operate in multiple bands have been developed. One family of such antennas, the planar-inverted F antennas (PIFAs), is particularly interesting due to their low profile, light weight, and conformal structure.

In this thesis a new multiband single-feed planar inverted-F dual-L antenna (PIFDLA) with overall size of  $24 \text{ mm} \times 30 \text{ mm} \times 7 \text{ mm}$  mounted on a  $30 \text{ mm} \times 30 \text{ mm} \times 1 \text{ mm}$  finite ground plane, is presented. The simulation for this multiband single-feed antenna has been carried out using HFSS software to investigate the antenna's performance and characteristics. From the simulation results, it has been found that the antenna is able to operate at the desired resonant frequencies for the lower band (2.4 GHz-2.63 GHz) and for the upper band (5.04 GHz-6.04 GHz) or for the lower band (2.47 GHz-2.74 GHz) and for the upper band (4.9 GHz-6.1 GHz) -depending on its height-, so this antenna at return loss of -10 dB fully covers Bluetooth band (2.4 GHz-2.4835 GHz) or WiMAX band (2.5 GHz-2.7 GHz)-depending on its height-, in addition to IEEE 802.11a (5.15 GHz-5.35 GHz, 5.725 GHz-

5.825 GHz) band, and HIPERLAN2 (5.47 GHz-5.725 GHz) band. Also the radiation pattern for this antenna is omidirectional.

Further study on this antenna needs to be carried out in order to prove that it is feasible, and can be used on WLAN mobile terminals. This includes the development of this antenna to verify its characteristics and performance, to study its performance with human interaction and investigate the Specific Absorption Rate (SAR) distribution in a human model.

## REFERENCES

- Azad M.Z. and Ali M., (2006), “**A New Class of Miniature Embedded Inverted-F Antennas (IFAs) for 2.4 GHz WLAN Applications,**” IEEE Trans. Antennas Propag. vol. 54, pp. 2585-2592.
- Balanis A., (1982) “**Antenna Theory Analysis and Design,**” John Wiley and Sons.
- Hirisawa K., Haneishi M., (1992), “**Analysis, Design, and Measurement of small and low-profile Antennas,**” Artech House, Boston.
- Janapsatya J., Esselle P., and Bird T.S., (2008), “**A Dual-Band and Wide-Band Planar Inverted-F Antenna for WLAN applications,**” Micro. Opt. Technol. Lett., vol.50, pp.138-141.
- Kathleen L. V., and Yahya R. S., 1997,” **Low-Profile Enhanced-Bandwidth PIFA Antennas for Wireless Communications Packaging,**” IEEE Trans. Antenna Propag. Vol. 45, PP. 1879-1888.
- Kevin R., B., and Leo P.L., 2006,”**Radiating and Balanced Mode Analysis of PIFA Antennas,**” IEEE Trans. Antenna Propag. Vol. 54, PP. 231-237.
- Looi C.K., and Terence S.P., and Chen Z.N.,”**Study of Human Effects on the Planar Inverted-F Antenna,**” Department of Electrical and Computer Engineering, National University of Singapore.
- Minh C. H., 2000, “**A Numerical and Experimental Investigation of PIFAs for Wireless Communication Applications,**” Virginia Polytechnic Institute of State University.
- Mueiz E. A., 2006, “**Multi-Band Antenna for GSM, 3G, Bluetooth and Wireless LAN Application,**” Department of Electrical Engineering, University of technology, Malaysia.
- Nepa P., Manara G., Serra A.A., and Nenna G., 2005, “**Multiband PIFA for WLAN Mobile Terminals,**” IEEE Antennas and Wireless Propagation Letters, Vol. 4, PP. 349-350.
- Olmos M.,Carrasco H.,Feick R., and Hirstov D.,2004,” **PIFA Input Bandwidth Enhancement by Changing Feed Plate Silhouette,**” Electron. Lett., Vol. 40, PP. 921-922.
- See C.H., Abd-Alhameed R.A., Zhou D., and Excell P.S., 2008, “**Dual-Frequency Planar Inverted F-L Antenna (PIFLA) for WLAN and Short Range Communication Systems,**” IEEE Trans. Antenna Propag. Vol. 56, PP. 3318-3320.

Wang Y.S., Lee M.C, and Chung S.J.,(2007), “ **Two PIFA-Related Miniaturized Dual-Band antennas,**” IEEE Trans. Antenna Propag., Vol. 55, pp.805-811.

## هوائي $F$ المقلوب المستوي المحسن ذو النطاقين لتطبيقات WLAN

اعداد

سناء فايق عارف سلامة

المشرف

الأستاذ الدكتور محمد كامل عبد العزيز

ملخص

شهدت الشبكات المحلية اللاسلكية التي تنتقل المعلومات بين الحواسيب نموا ملحوظا وأصبح تصميم أجهزة تعمل على الترددات المخصصة لتطبيقات الشبكات المحلية اللاسلكية موضوع البحث وذلك من خلال احتوائها على هوائيات متعددة النطاق لتغطية تطبيقات الشبكات المحلية اللاسلكية، بالإضافة الى أن صغر المساحة المتاحة في الهواتف والحواسيب المحمولة جعلت من الضروري التوجه الى تصميم هوائيات صغيرة الحجم، خفيفة الوزن، وتغطي أكثر من تطبيق بدلا من استعمال هوائي لكل تطبيق .

يعد هوائي المقلوب المستوي من أشهر الهوائيات المستخدمة في الهواتف والحواسيب المحمولة لصغر حجمه وخفة وزنه وامكانية تعديله لتغطية أكثر من نطاق وفي هذه الرسالة سيقدم هوائي  $F$  المقلوب المستوي متعدد النطاقات لتغطية تطبيقات الشبكات المحلية اللاسلكية.

لقد حلل هذا الهوائي باستعمال برمجية HFSS لتوضيح خصائصه وكفاءته، وأوضحت النتائج أن هذا الهوائي قادر على تغطية تطبيقات الشبكات المحلية اللاسلكية IEEE802.11a/b/g، البلوتوث، و HIPERLAN2 .